AD-A084 230 WEAPONS SYSTEMS RESEARCH LAB ADELAIDE (AUSTRALIA) F/G 20/4
WIND TUNNEL TESTS OF A SPINNING 105 MM ARTILLERY SHELL MODEL WI--ETC(U)
SEP 79 C JERMEY
UNCLASSIFIED WSRL-0122-TR NL

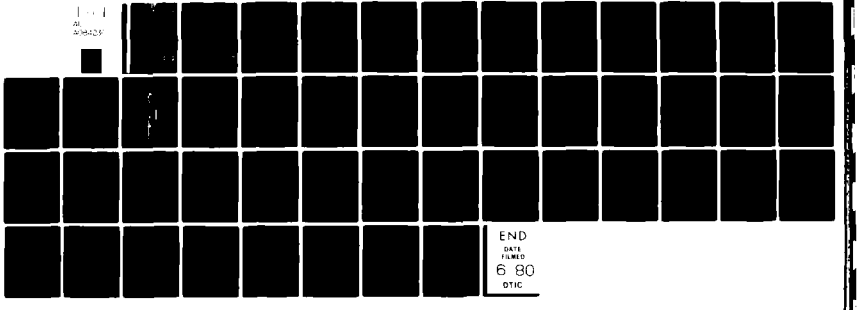

END
DATE FILMED
6 80
DTIC

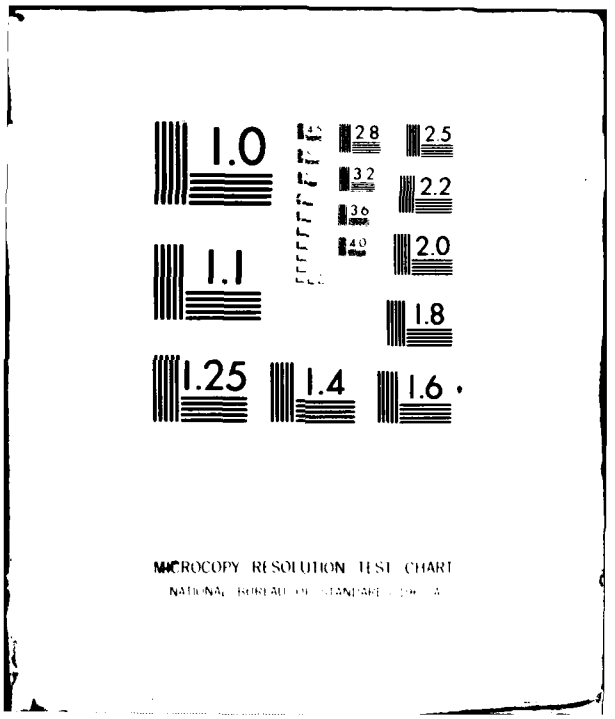
1.0
1.1
1.25
1.4
1.6
2.8
3.2
3.6
4.0
2.5
2.2
2.0
1.8
MICROCOPY RESOLUTION TEST CHART
NATIONAL BUREAU OF STANDARDS - 1963 - A

WSRL-0122-TR

AR-001-908

DEPARTMENT OF DEFENCE

DEFENCE SCIENCE AND TECHNOLOGY ORGANISATION

WEAPONS SYSTEMS RESEARCH LABORATORY

DEFENCE RESEARCH CENTRE SALISBURY
SOUTH AUSTRALIA

TECHNICAL REPORT
WSRL-0122-TR

WIND TUNNEL TESTS OF A SPINNING 105 mm ARTILLERY SHELL MODEL WITH CANARD CONTROL SURFACES

C. JERMEY

Approved for Public Release

SEPTEMBER 1979

UNCLASSIFIED

AR-001-908

DEPARTMENT OF DEFENCE

DEFENCE SCIENCE AND TECHNOLOGY ORGANISATION

WEAPONS SYSTEMS RESEARCH LABORATORY

(9) TECHNICAL REPORT

(14) WSRL-0122-TR

(6) WIND TUNNEL TESTS OF A SPINNING 105 mm ARTILLERY SHELL MODEL WITH CANARD CONTROL SURFACES

(10) C./Jermey

(11) Sep 79

SUMMARY (12) 51

Tests have been conducted to measure the aerodynamic characteristics of a spinning model of a 105 mm shell fitted with canard control surfaces. The tests covered an incidence range of -2^{o} to 15^{o}, a Mach number range of 0.70 to 0.95, and a control deflection range of zero to 30^{o}. The effectiveness of the canards as pitch and yaw controls and for generating manoeuvring forces is discussed. The conclusion is reached that available manoeuvring forces would be small, and an example is given for a typical trajectory in which a maximum shift of 90 m from the unguided impact point could be obtained.

Approved for Public Release

POSTAL ADDRESS: Chief Superintendent, Weapons Systems Research Laboratory, Box 2151, G.P.O., Adelaide, South Australia, 5001.

DOCUMENT CONTROL DATA SHEET

Security classification of this page: UNCLASSIFIED

1 DOCUMENT NUMBERS	2 SECURITY CLASSIFICATION
AR Number: AR-001-908	a. Complete Document: Unclassified
Report Number: WSRL-0122-TR ✓	b. Title in Isolation: Unclassified
Other Numbers:	c. Summary in Isolation: Unclassified

3 TITLE

WIND TUNNEL TESTS OF A SPINNING 105 mm ARTILLERY SHELL MODEL WITH CANARD CONTROL SURFACES

4 PERSONAL AUTHOR(S):	5 DOCUMENT DATE:
C. Jermey	September 1979
	6 6.1 TOTAL NUMBER OF PAGES 40
	6.2 NUMBER OF REFERENCES: 2

7 7.1 CORPORATE AUTHOR(S):	8 REFERENCE NUMBERS
Weapons Systems Research Laboratory	a. Task: DST 77/031
7.2 DOCUMENT SERIES AND NUMBER ✓ Weapons Systems Research Laboratory 0122-TR	b. Sponsoring Agency:
	9 COST CODE: 330834

10 IMPRINT (Publishing organisation)	11 COMPUTER PROGRAM(S) (Title(s) and language(s))
Defence Research Centre Salisbury	

12 RELEASE LIMITATIONS (of the document):

Approved for Public Release

12.0	OVERSEAS	NO		P.R.	1	A		B		C		D		E	

Security classification of this page: UNCLASSIFIED

Security classification of this page: UNCLASSIFIED

13 ANNOUNCEMENT LIMITATIONS (of the information on these pages):

No limitation

14 DESCRIPTORS:

a. EJC Thesaurus Terms

105 mm shells
Projectiles
Spinning projectiles
Spin stabilised ammunition
Wind tunnel tests
Canard controls

b. Non-Thesaurus Terms

15 COSATI CODES:

16 LIBRARY LOCATION CODES (for libraries listed in the distribution):

17 SUMMARY OR ABSTRACT:
(if this is security classified, the announcement of this report will be similarly classified)

Tests have been conducted to measure the aerodynamic characteristics of a spinning model of a 105 mm shell fitted with canard control surfaces. The tests covered an incidence range of -2° to 15°, a Mach number range of 0.70 to 0.95, and a control deflection range of zero to 30°. The effectiveness of the canards as pitch and yaw controls and for generating manoeuvring forces is discussed. The conclusion is reached that available manoeuvring forces would be small, and an example is given for a typical trajectory in which a maximum shift of 90 m from the unguided impact point could be obtained.

Security classification of this page: UNCLASSIFIED

TABLE OF CONTENTS

LIST OF FIGURES

12. Variation of yawing moment coefficient with incidence and yaw canard deflection, $p' = 0$, $\delta_z = 0^o$

13. Variation of aerodynamic coefficients with incidence, showing effect of pitch and yaw canard deflections applied separately and in combination, $M = 0.7$, $p' = 0$

14. Variation of aerodynamic coefficients with spin rate, showing effect of pitch and yaw canard deflections, $M = 0.7$, $\alpha = 5^o$

15. Variation of trim incidence with pitch canard deflection and Mach No., $p' = 0$, $\delta_y = 0^o$

16. Variation of normal force and side force coefficients with trim incidence and Mach No.

1. INTRODUCTION

The work reported here was carried out during February 1978 as part of a programme to assess the effectiveness of canard surfaces in controlling the flight path of a spin stabilised projectile. The baseline projectile shape chosen for investigation was the 105 mm M1 artillery shell, and an earlier series of wind tunnel tests conducted on this standard shape are reported by Jermey in reference 1. The tests reported here used, as far as possible, the same model, systems and techniques as already detailed in reference 1. Therefore, except where significant differences existed, detailed description of the model, drive system and experimental techniques are not included in this report. A theoretical study of the effectiveness of canard controls on the 105 mm shell has also been conducted by Brown, Hunter and Lloyd and is reported by them in reference 2. Conclusions from both references 1 and 2 suggest that canard surfaces do not appear to offer very high manoeuvrability in subsonic and transonic flight; in particular, Brown et al estimate a flight path deviation of approximately 80 m for a manoeuvring phase lasting 16 s at Mach 0.75. The present experimental work generally confirms this conclusion. For the parameters given above (16 s manoeuvre at Mach 0.75) the experimental data give a maximum flight path deviation of approximately 90 m.

2. EXPERIMENTAL DETAILS

2.1 Model and balance

The basic model was the half scale 105 mm HE M1 shell model built for the earlier test series(ref.1). To assess the canard effectiveness in a realistic way the nose of the shell was redesigned to conform with the control section geometry then under consideration. Figures 1 and 2 show the model and balance assembly, and it can be seen that the nose section is somewhat blunter and more bulbous than that of the standard shell. The modifications consist of the removal of the standard fuse and the addition of two separate pieces, a non-spinning control section which contains the two canard pairs, and a thin walled shell which fairs the control section back into the body and which spins with the shell body.

The control section is mounted on a shaft which passes through the hollow core of the air motor and keys into the model support sting to prevent rotation. Lateral support is provided by ball bearings between the shaft and the shell body. For a more detailed description of the model support and drive system the reader is referred to reference 1.

2.2 Experimental procedure

All tests were conducted in the 360 mm x 380 mm slotted working section of the continuous flow wind tunnel S-1 at the Aeroballistics Division of WSRL. Four component data (no drag or rolling moment) were obtained for a Mach number range of 0.70 to 0.95, an incidence range of -2^{o} to 15^{o}, and for control deflections from 0^{o} to 30^{o}. No supersonic runs were conducted as the terminal speed of the shell is subsonic for all trajectories in which terminal guidance could be employed. A Reynolds number of $R_d = 3.9 \times 10^5$ (based on maximum body diameter) was used for all tests, which compares with flight Reynolds numbers of 1.0 to 2.0×10^6. To simulate the flow conditions expected at the higher Reynolds numbers of the full scale shell, a boundary layer trip, shown in figure 1, was used to ensure a turbulent boundary layer over the shell body.

For further details of the conduct of the individual wind tunnel tests the reader is referred to reference 1.

2.3 Accuracy of results

Reference 1 discusses most of the sources of error in the present results, so those items which are common to both reference 1 and the present work are simply identified below and the accuracy applicable to each is given. The setting of control surface deflections is the only feature not present in reference 1, and so this is discussed in some detail.

(a) Force and moment coefficients: ± 0.01, ± 1%

(b) Mach number: ± 0.01

(c) Reynolds number: all tests within range $(3.9 \pm 0.1) \times 10^5$

(d) Incidence: $\pm 0.2^{\circ}$

(e) Roll rate: for each data point ± 6 rad/s

for an entire incidence traverse ± 19 rad/s

(f) Control deflections:

The angular deflection of each canard was set by driving the model to a predetermined attitude and then setting the canard top rear surface level by the use of a dial indicator referenced to the bottom tunnel liner. Each canard was individually set and then locked in position prior to each series of runs, the canard angular deflection being given by the model pitch angle plus the half angle of the canard rear surface ($1\frac{1}{2}^{\circ}$). Uncertainties arising in this setting technique include the model attitude (readout errors and sting bending due to tare effects), inclination of the tunnel liner surface, and dimensional uncertainty of the individual canards. Nominal accuracy for the setting of each canard was 0.1°, and the cumulative effect of the remaining errors amounts to an additional 0.15°, so an uncertainty of $\pm 0.25^{\circ}$ can be assumed for each given deflection.

3. PRESENTATION AND DISCUSSION OF RESULTS

All results are referred to the axis system shown in figure 3, the origin of the system being located at the nominal centre of gravity of the standard shell. Only graphical results are presented, data having been selected to illustrate the aerodynamic aspects of interest. A tabulation of the complete aerodynamic data is available, however, and may be obtained on request to the author.

3.1 Effects of canards and spin rate

Figures 4, 5 and 6 show respectively, the centre of pressure, normal force and pitching moment coefficients versus incidence for the model both with and without the canards attached. These results are given only for zero spin rate since their variation with spin rate is small. The centre of pressure without canards is further forward than for the standard shell (attributable to the longer and blunter nose shape) and shows the normal effect of forward movement with increasing Mach number and rearward movement with increasing incidence. The addition of the canards, with their lift contribution occurring at a relatively constant position, stabilises the centre of pressure somewhat, reducing its variability with Mach number and incidence. Normal force coefficients without canards (figure 5(a)) are very similar to those of the standard shell shape. The addition of canards (figure 5(b)) increases normal force coefficients by approximately 50% throughout the Mach number and incidence range. Pitching moment coefficients (figure 6) follow the same pattern, except that the model without canards is more unstable than the standard shell shape due to the further forward centre of pressure. The addition of canards further destabilises the model, moments on the canard equipped model being approximately 70% greater than those on the standard shell shape.

Figures 7 and 8 show the side force and yawing moment coefficients versus incidence with and without canards, plus the effect of varying spin rate (given in non-dimensional form). All data show a zero shift, small for the model with no canards, and greater for the canard equipped case. This is most likely due mainly to non-axial airflow in the tunnel working section and possibly also to small errors in the setting of the canards. As a result, absolute values of coefficients may be significantly in error (although within the limits as given in Section 2.3) but trends with incidence and roll rate should be reliable. Once again, results for the model with no canards agree closely with earlier results from the standard shell shape. The addition of canards generally has very little effect in the low incidence (up to 10^{o}) range, but appears to produce a small to moderate increase in Magnus forces and moments at higher incidences.

3.2 Effects of pitch canard deflection

Pitch canard deflections ranged from 0^{o} up to 30^{o}, and their effect on normal force and pitching moment coefficients is shown in figures 9 and 10. The two unusual deflection angles, 13^{o} and 23^{o}, were the unfortunate result of a 3^{o} setting error present when setting to nominal angles of 10^{o} and 20^{o}. The error was discovered during the test series, but too late to conduct repeat runs at the originally intended angles. Results are plotted only for zero spin rate and two Mach numbers, 0.7 and 0.95, since the variation with spin rate and Mach number is small. Figures 9 and 10 show that normal force and pitching moments vary relatively linearly throughout the incidence range for pitch canard deflections of up to 23^{o}. The curves for 30^{o} deflection indicate that stalling of the canard surfaces commences at a canard to free stream incidence of approximately 25^{o} (i.e., in this case, at 5^{o} body incidence) and worsens progressively for higher canard to freestream angles. Pitching moment curves show that trim angles of up to $5\frac{1}{2}^{o}$ (spin-stabilised) can be obtained with canard deflections of up to 30^{o}. A more detailed discussion of trim angles and normal force available at trim is given in Section 3.6.

3.3 Effects of yaw canard deflection

Yaw canard deflections ranged from 0^{o} to 30^{o}, and their effect on side force and yawing moment coefficients is shown in figures 11 and 12. Plotted results are given only for zero spin rate and two Mach numbers, 0.7 and 0.95. Results at other Mach numbers are similar, and the effect of spin rate is covered separately (see Section 3.5). The effectiveness of canard deflections in producing side forces and yawing moments appears to be fairly linear with δ_y for deflections up to 20^{o}, but it is evident that, as for the pitch canards, stalling is occurring at a deflection of 30^{o}. Side forces due to canard deflection are significantly increased by increasing incidence, though yawing moments remain fairly constant, implying a rearward shift of the $C.P._y$ position with incidence.

3.4 Combined effects of pitch and yaw canard deflections

A single series of tests was conducted to check whether the effects of pitch and yaw canard deflections applied simultaneously were significantly different from their separate effects. Figure 13 shows normal force, pitching moment, side force and yawing moment coefficients obtained for four permutations of pitch and yaw canard deflections (plotted results for $\delta_z = 20^{o}$, $\delta_y = 0^{o}$ were obtained by linear interpolation between the test results $\delta_z = 13^{o}$, $\delta_y = 0^{o}$ and $\delta_z = 23^{o}$, $\delta_y = 0^{o}$). Plots are given only for $M = 0.7$ and zero spin rate, but results are similar for other Mach numbers and spin rates. Results indicate that cross coupling effects, i.e. C_Z and C_m changes produced by δ_y, and C_Y and C_n changes produced by δ_z, are small.

Thus the effect of simultaneous application of pitch and yaw canards is little or no different to the simple addition of their separate effects.

3.5 Combined effects of spin rate with pitch and yaw canard deflections

Figure 14 shows plotted results of normal force, pitching moment, side force and yawing moment coefficients versus non-dimensional spin rate (p') for various control surface deflections. Data are plotted only for an incidence of 5^{o} (approximately the maximum trim incidence attainable, see Section 3.6) and for Mach 0.7. Results for the rest of the Mach number range are similar. Figures 14(a) and (b) show that spin rate has no significant effect on normal force or pitching moment, the small perturbations which do appear being within the limits of experimental uncertainty. Figures 14(c) and (d) show that spin rate and yaw canard deflection also have largely independent effects, although there is some indication that the Magnus component of the side force is slightly increased by canard deflection, but again, the increment is at the limit of experimental uncertainty.

3.6 Trim incidence and manoeuvring forces at trim

Figure 15 shows the trim incidence available throughout the Mach number range for pitch canard deflections of 0^{o} to 30^{o}. An incidence of up to $5\frac{1}{2}^{o}$ is possible (with the assumption of gyroscopic stability) and, within the range tested, trim is independent of Mach number and an almost linear function of canard deflection.

The normal force coefficient produced at trim is shown in figure 16(a). It can be seen that the normal force is very small and an extremely non-linear function of both trim incidence and Mach number. This disappointing result is due to the proximity of the centre of pressure of the body lift to the canard position, which means that to obtain trim at incidence the canard lift force must be opposite and almost equal to the body lift. The resultant total lift is very small, and highly dependent on the changes in the body centre of pressure caused by Mach number and incidence changes.

The side force coefficient at trim, shown in figure 16(b), consists mainly of the Magnus component, but also contains a small yaw canard force required to balance the Magnus moment about the centre of gravity. The total side force coefficient is thus a relatively simple function of spin rate and trim incidence, but even at maximum incidence side forces are very small for all practical Mach numbers and spin rates. The significant zero offsets present on figures 16(a) and (b) result from the difficulties of accurately measuring these small force levels.

The total manoeuvring force on the shell is obtained from a vector addition of the normal and side force components. Thus, for a range of realistic Mach numbers, spin rates and trim incidences, the manoeuvring force coefficient could range from zero to approximately 0.045, and could vary in direction through a range of at least 90^{o}. For example, taking Mach 0.75 and a spin rate of 160 rev/s ($p' \approx 0.11$) as typical of conditions at the end of a maximum range trajectory, the total manoeuvring force coefficient would be approximately 0.03 in a direction inclined at approximately 20^{o} to the incidence plane.

3.7 Concluding remarks

The use of canard surfaces to control the subsonic terminal trajectory of a spin stabilised projectile appears to be capable of only minor trajectory perturbations. For example, taking a mean Mach number of 0.75 and a spin rate of 160 rev/s as typical terminal conditions, the maximum available manoeuvrability is about 0.07 g. For a manoeuvring phase lasting 16 s (which assumes target detection at greater than 4 km range) the resulting trajectory deviation is approximately 90 m.

The disappointing performance results not from a lack of body lift but rather from the unfortunate juxtaposition of the body centre of pressure and the control surfaces. The canards are situated in close proximity to the aerodynamic centre of pressure of the body and therefore trim at incidence

is only maintained when the canard lift is opposite and almost equal to the body lift. The total available lift can therefore only be a small fraction of the body alone lift. The Magnus force, an additional possibility for producing trajectory deviations, is also small, being of a similar order of magnitude to the total lift force.

Improvements in manoeuvrability should be possible from any modification which produces a significant separation between the body lift and the control force. Thus, operation at supersonic speeds should give improved performance due to the more rearward centre of pressure of body lift. For the 105 mm shell considered here, however, a supersonic terminal speed is attainable only at extremely close ranges. Other options might include the addition of fixed tail fins to shift the centre of pressure rearward, or the replacement of the canard controls by tail controls, thus shifting the control force location rearward.

NOTATION

C_Z	normal force coefficient = $\frac{Z}{qS}$
C_Y	side force coefficient = $\frac{Y}{qS}$
C_m	pitching moment coefficient = $\frac{m}{qSd}$
C_n	yawing moment coefficient = $\frac{n}{qSd}$
$C.P._Z$	position of centre of pressure in the pitch plane, forward of cg is +ve
$C.P._y$	position of centre of pressure in the yaw plane, forward of cg is +ve
M	Mach number of free stream
R_d	Reynolds number of free stream, based on maximum body diameter
S	maximum body cross sectional area
U_∞	velocity of free stream
Y	side force
Z	normal force
d	maximum body diameter
m	pitching moment
n	yawing moment
p	spin rate; clockwise from rear is +ve
p'	non-dimensional spin rate = $\frac{pd}{2U_\infty}$
q	dynamic pressure of free stream
α	incidence angle relative to free stream
δ_y	deflection of yaw canards, positive when leading edge moves in Y axis direction
δ_z	deflection of pitch canards, positive when leading edge moves in Z axis direction

REFERENCES

No.	Author	Title
1	Jermey, C.	"Wind tunnel tests on the static aerodynamics of a spinning 105 mm artillery shell model". WSRL-0090-TR, March 1979
2	Brown, D.P., Hunter, J.S. and Lloyd, K.H.	"Calculations relating to the use of canards to terminally correct the trajectory of 105 mm shells". WRE-TM-1903 (W), November 1977

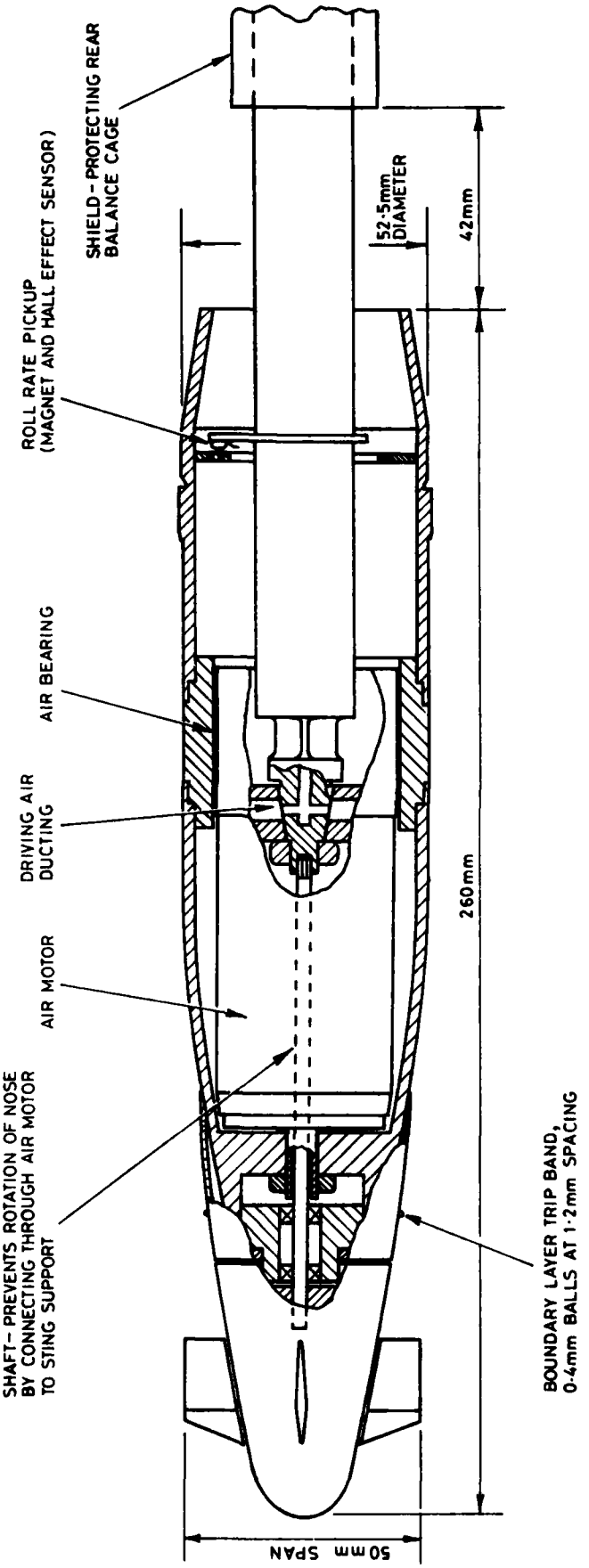

Figure 1. 105 mm canard controlled shell model, showing internal details

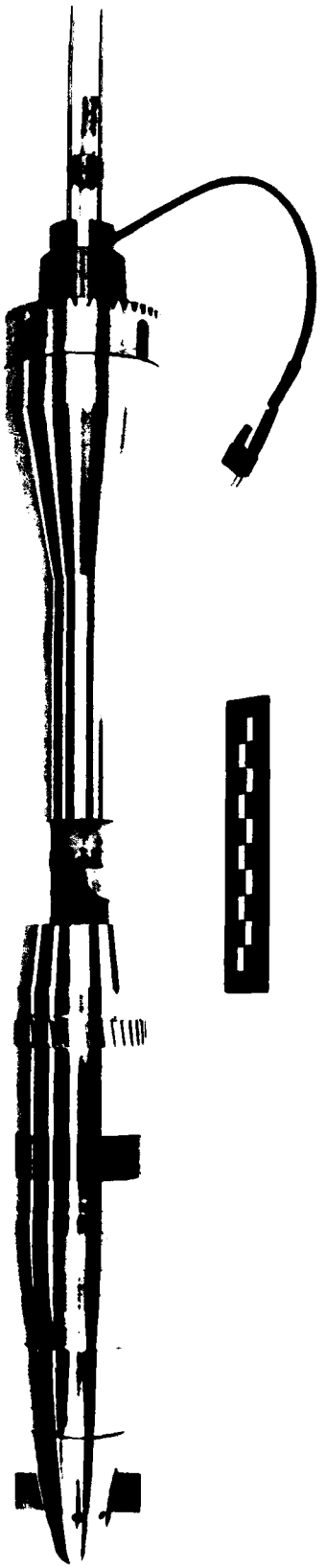

Figure 2. Assembly of model, balance and balance shield

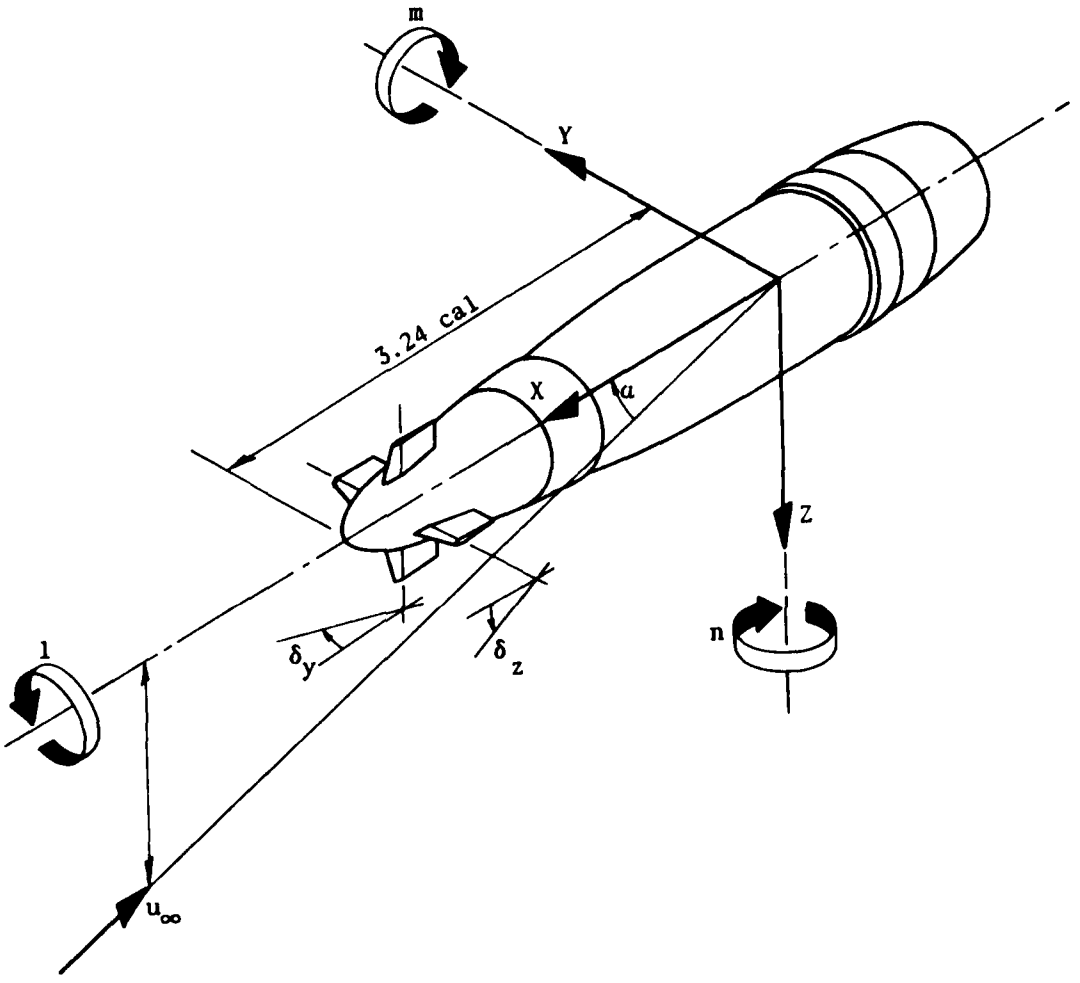

Figure 3. Axis system used in presentation of results

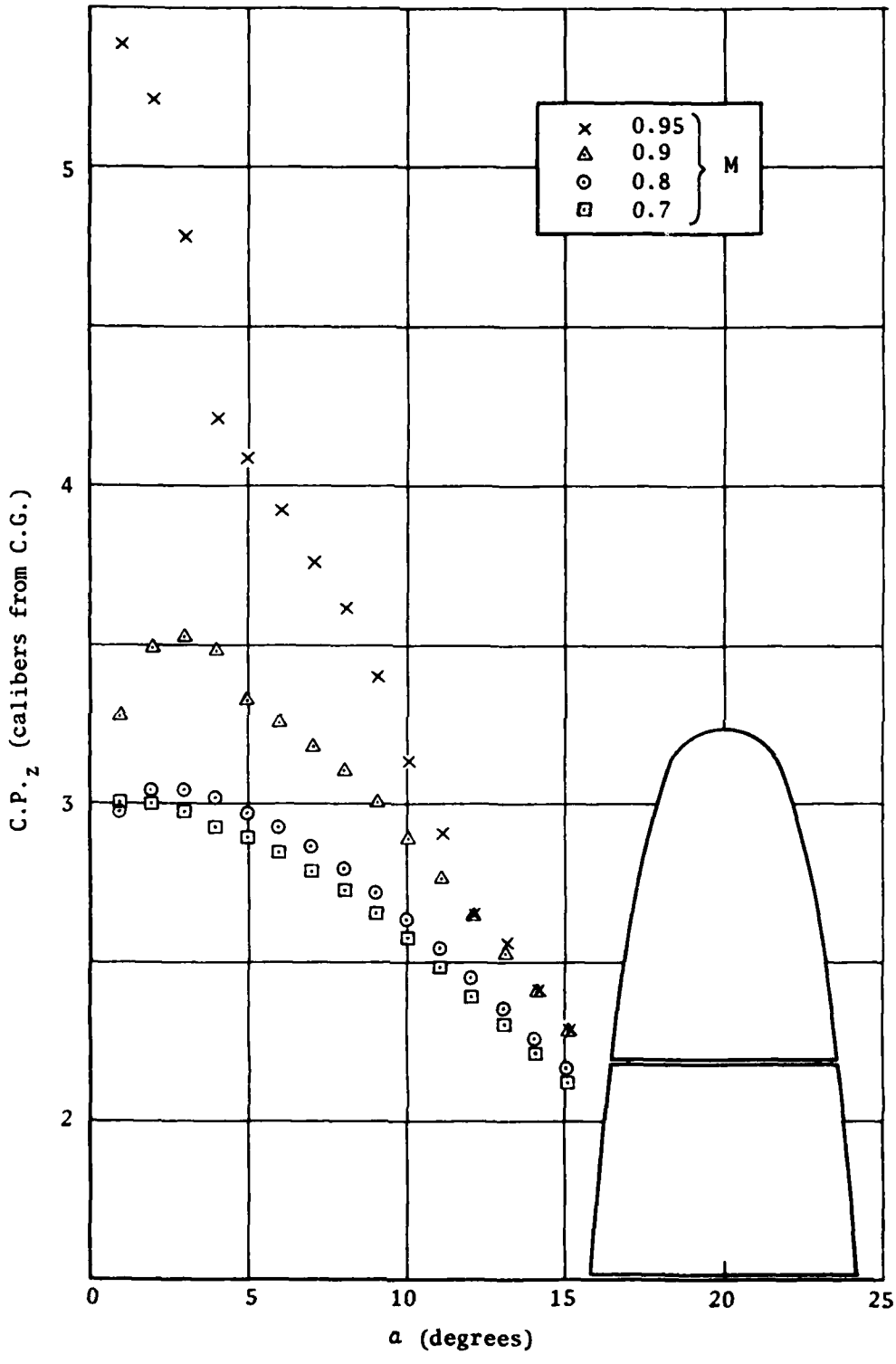

(a) No canards

Figure 4. Variation of centre of pressure in pitch plane with incidence and Mach No., $p' = 0$

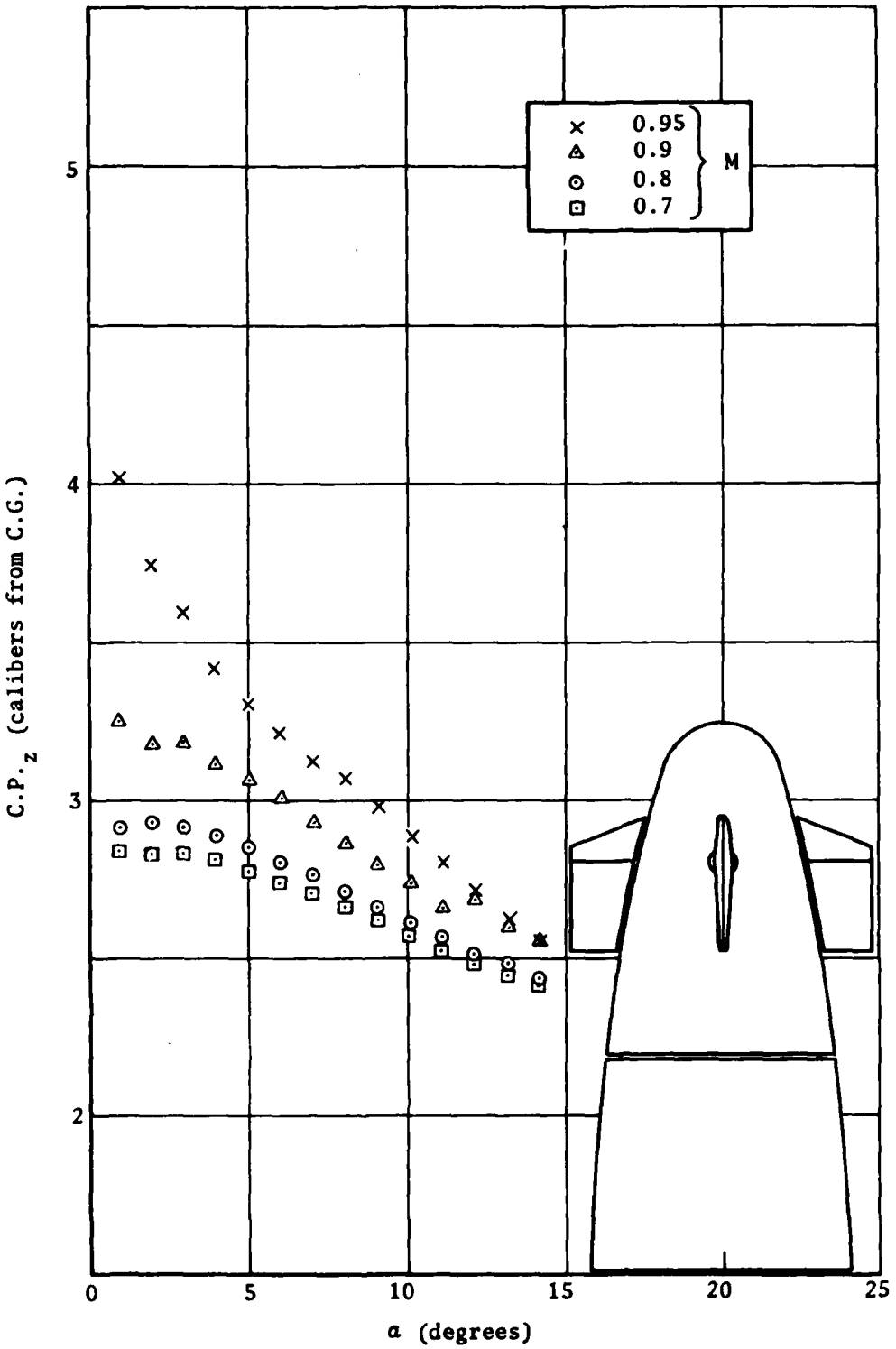

(b) With canards, $\delta_z = \delta_y = 0^o$

Figure 4(Contd.). Variation of centre of pressure in pitch plane with incidence and Mach No., $p' = 0$

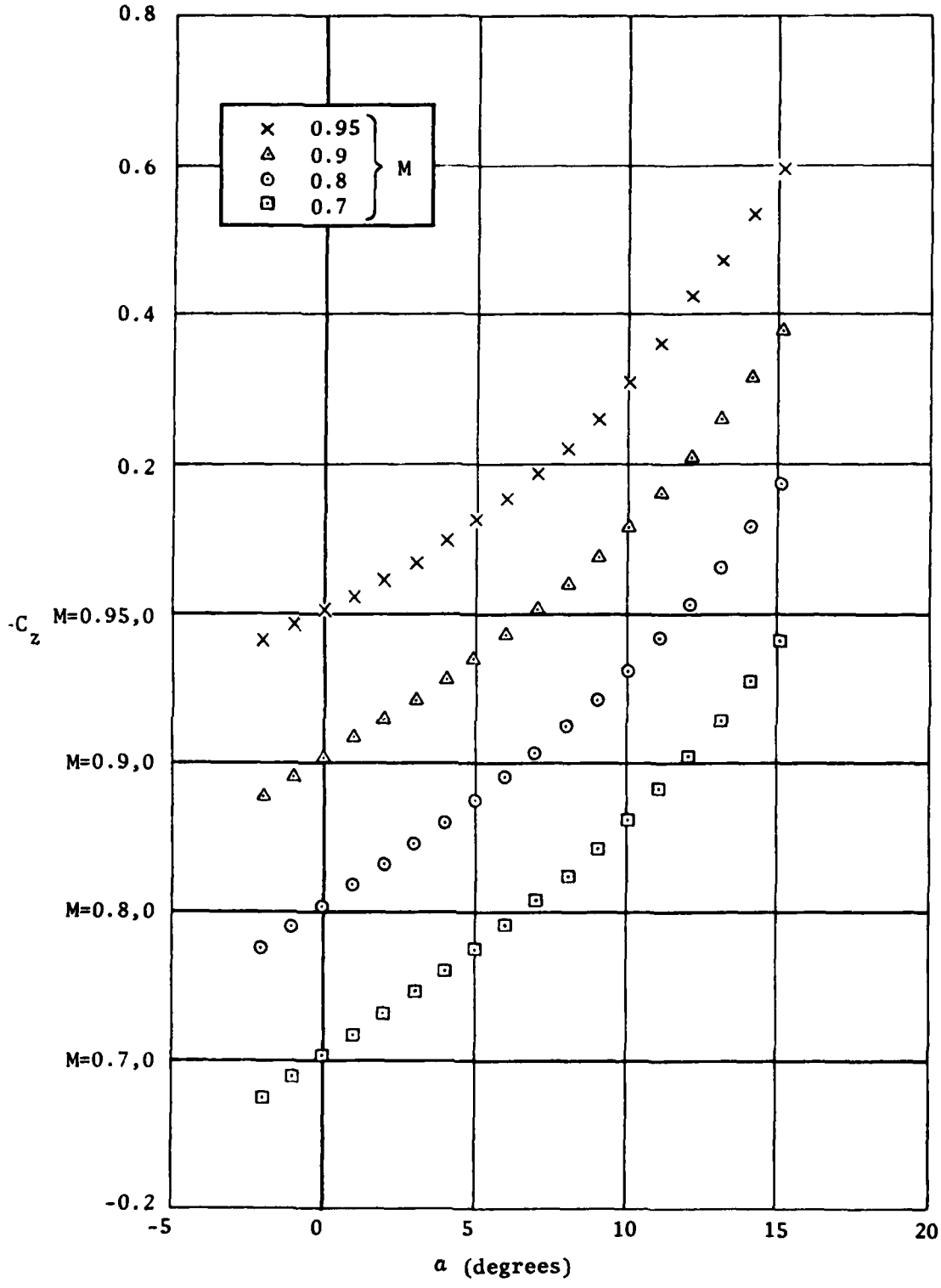

(a) No canards

Figure 5. Variation of normal force coefficient with incidence and Mach No., $p' = 0$

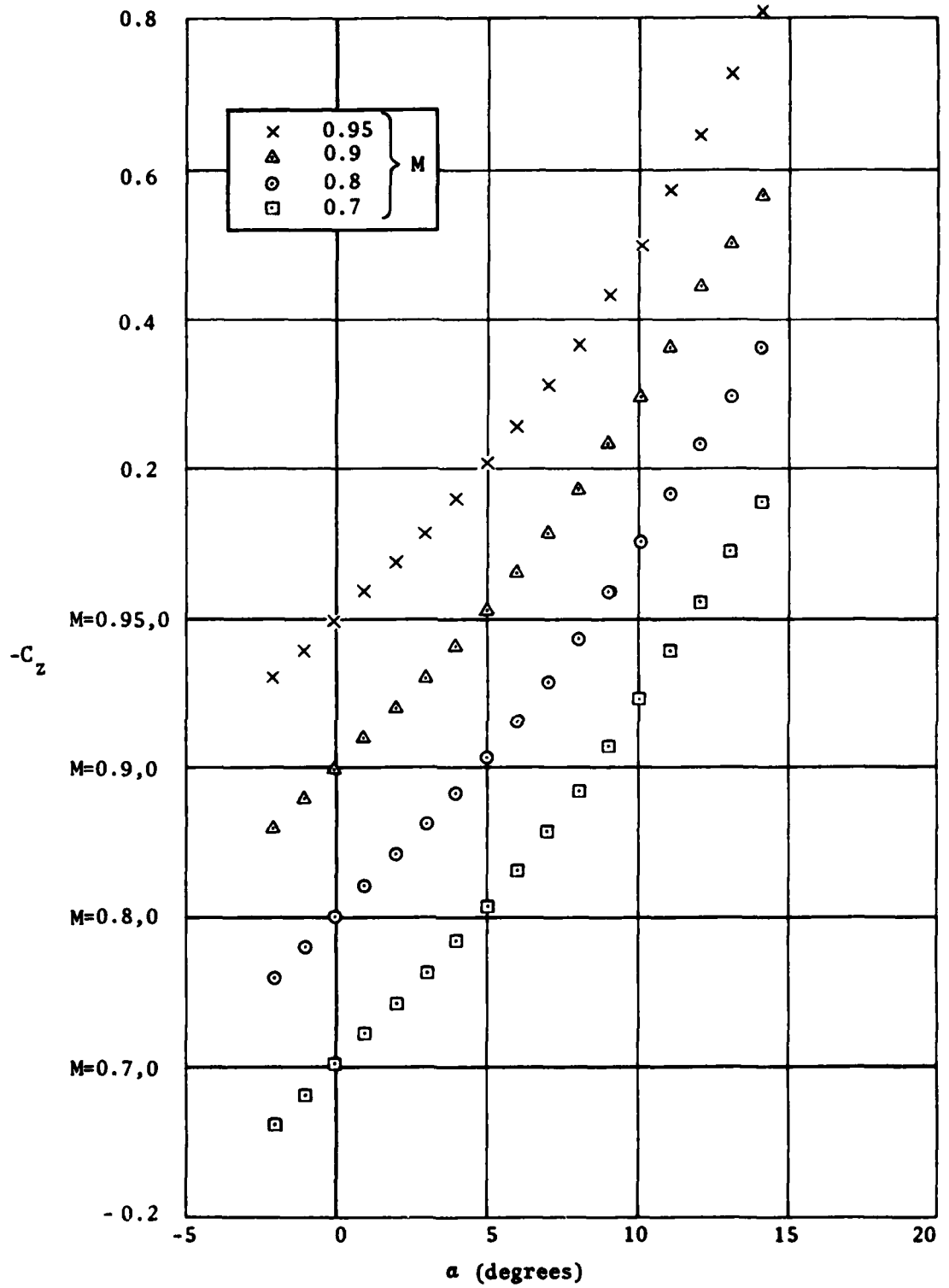

(b) With canards, $\delta_z = \delta_y = 0^o$

Figure 5(Contd.). Variation of normal force coefficient with incidence and Mach No., $p' = 0$

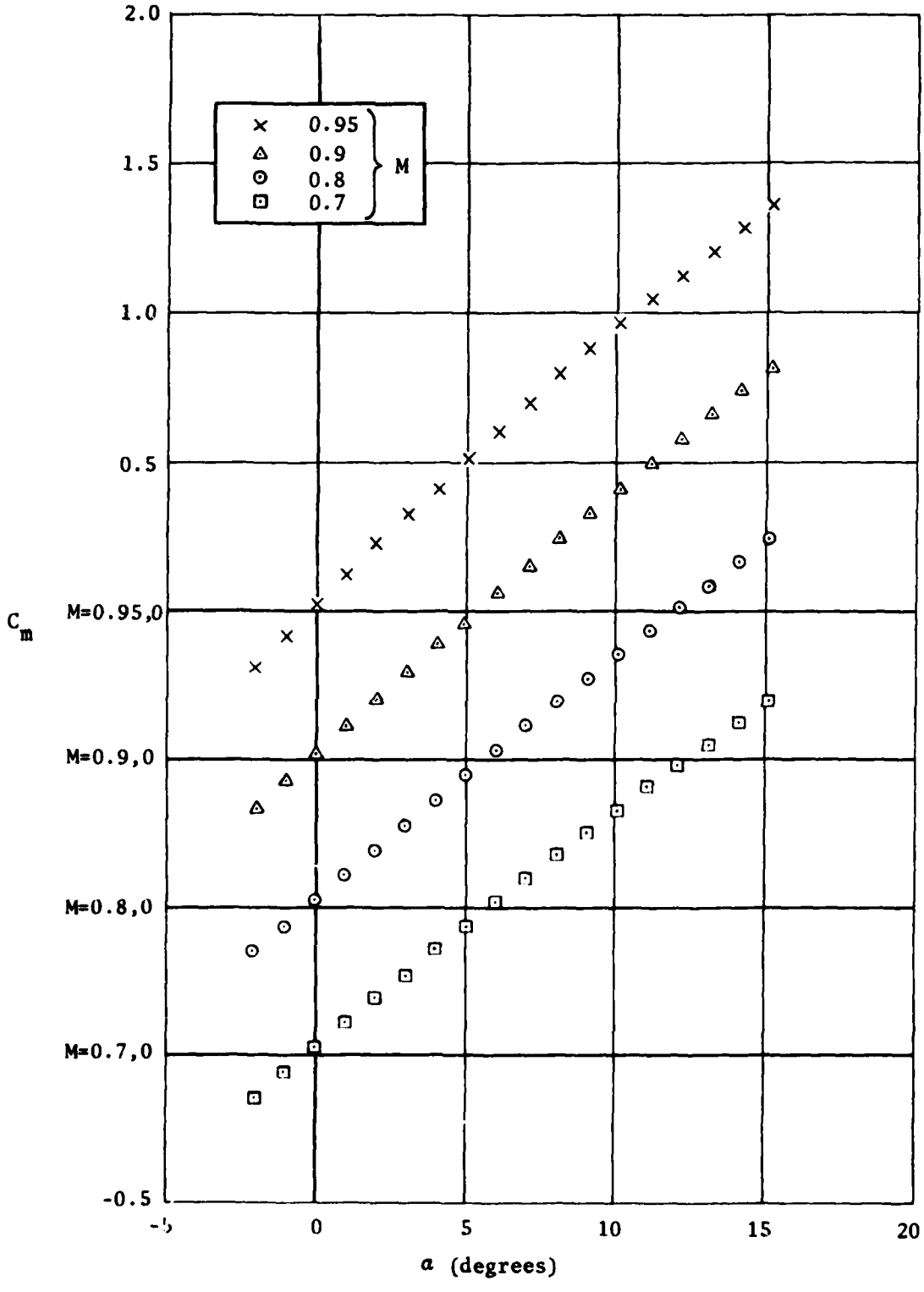

(a) No canards

Figure 6. Variation of pitching moment coefficient with incidence and Mach No., $p' = 0$

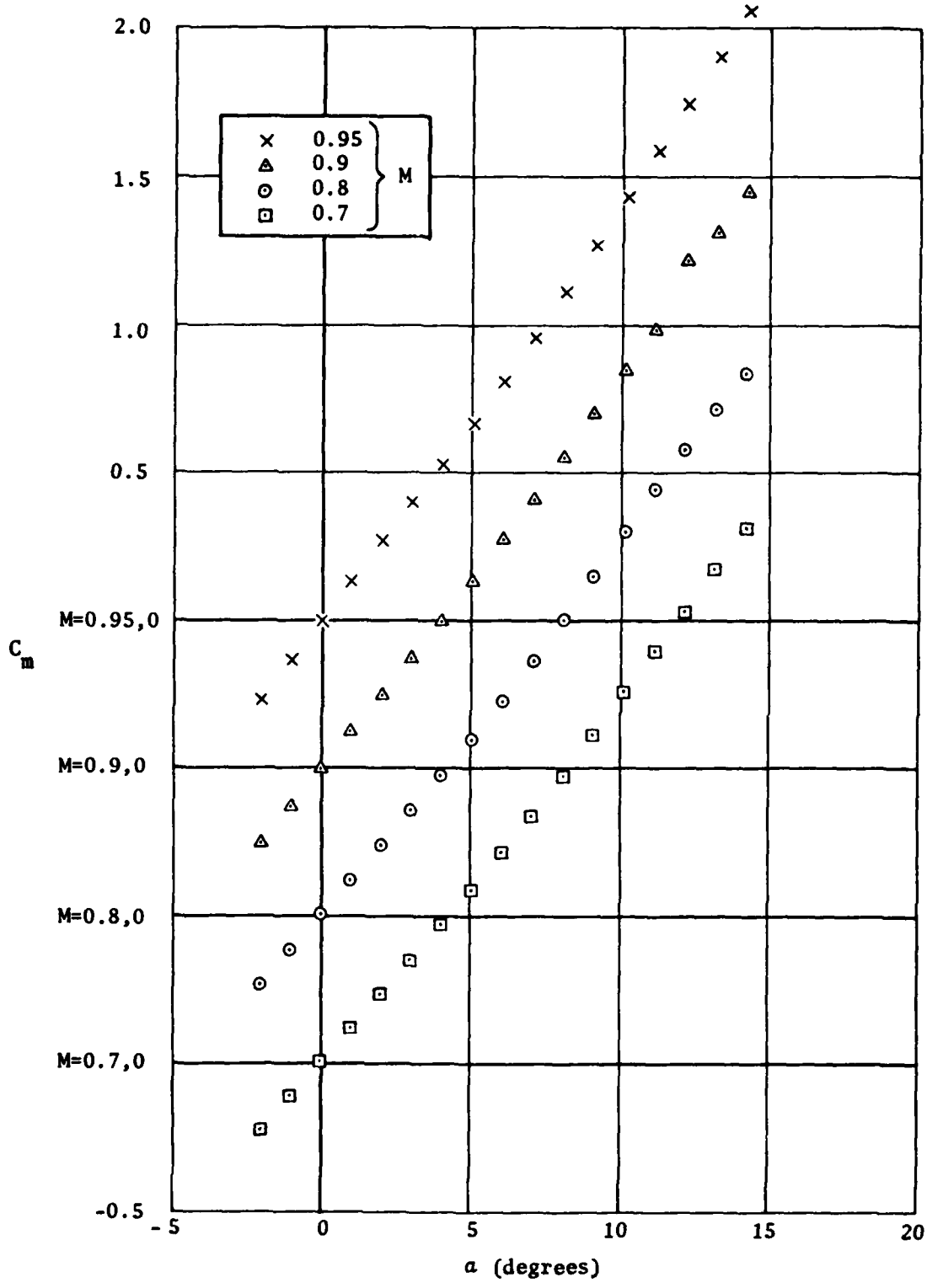

(b) With canards, $\delta_z = \delta_y = 0^o$

Figure 6(Contd.). Variation of pitching moment coefficient with incidence and Mach No., $p' = 0$

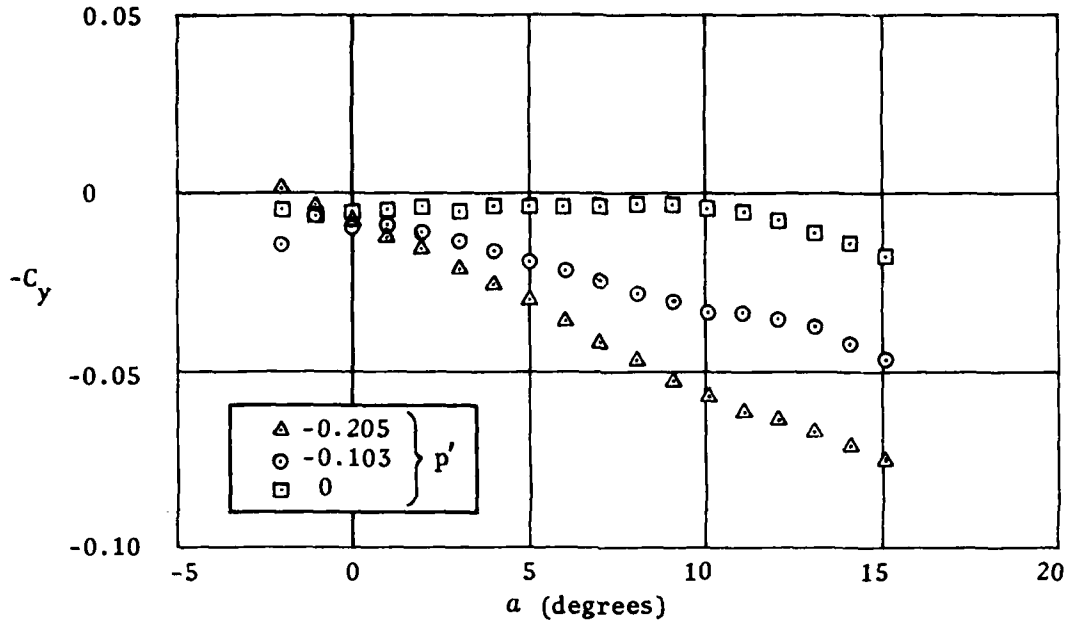

(a) M=0.7, no canards

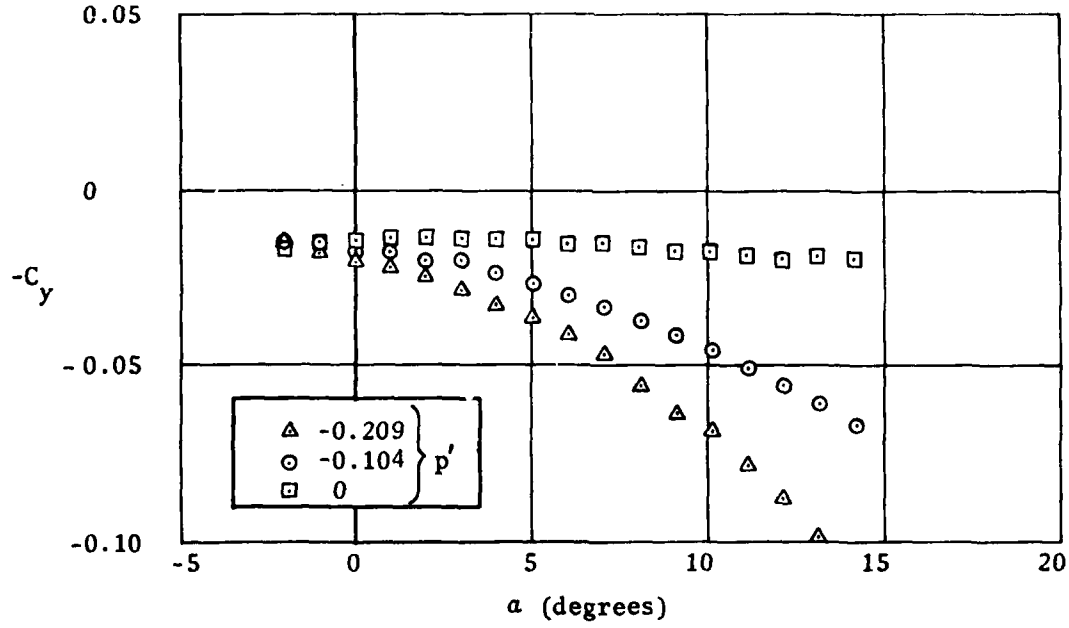

(b) M=0.7, with canards, $\delta_z = \delta_y = 0^o$

Figure 7. Variation of side force coefficient with incidence, Mach No. and spin rate

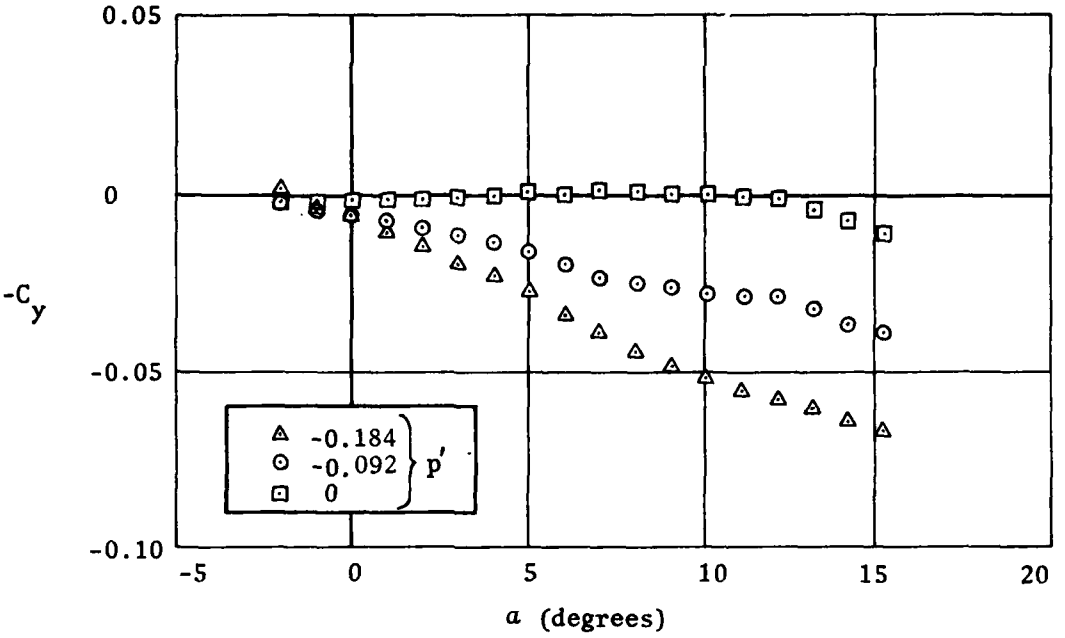

(c) M=0.8, no canards

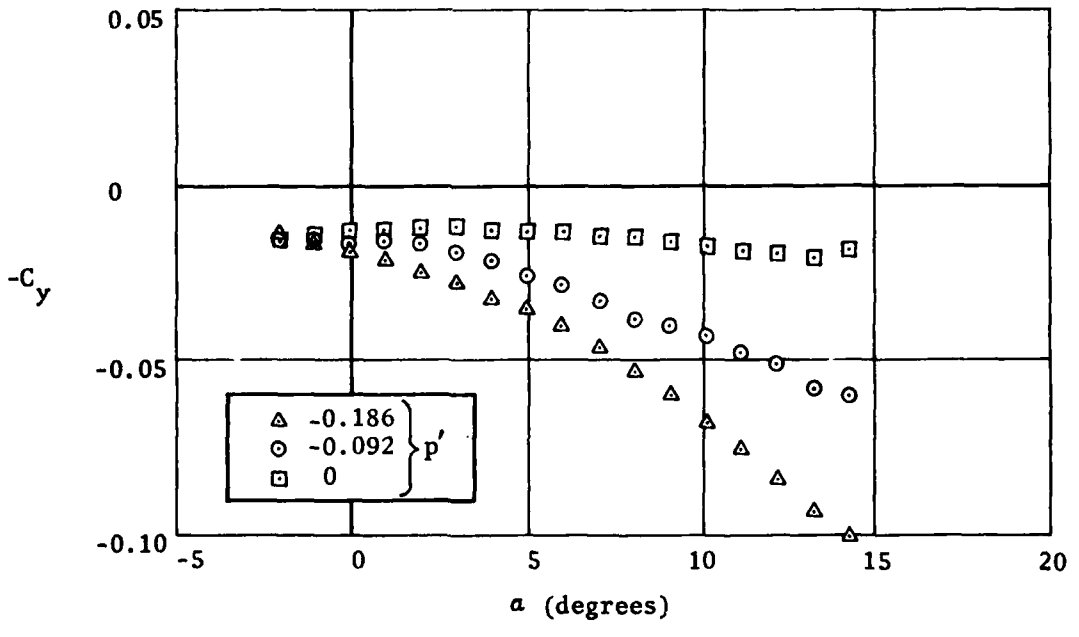

(d) M=0.8, with canards, $\delta_z = \delta_y = 0^o$

Figure 7(Contd.). Variation of side force coefficient with incidence, Mach No. and spin rate

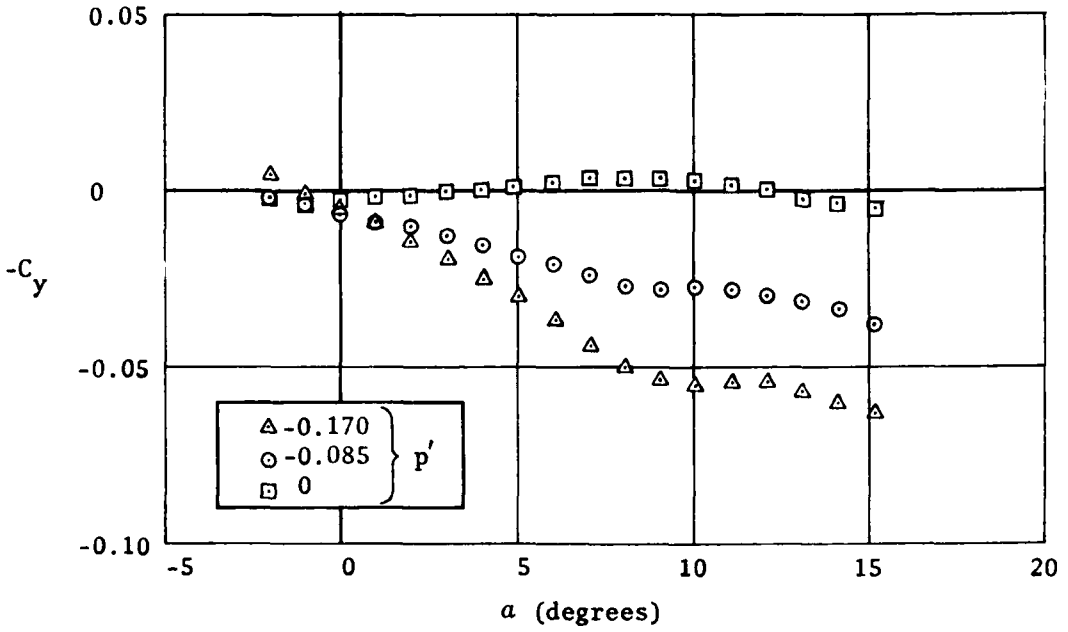

(e) M=0.9, no canards

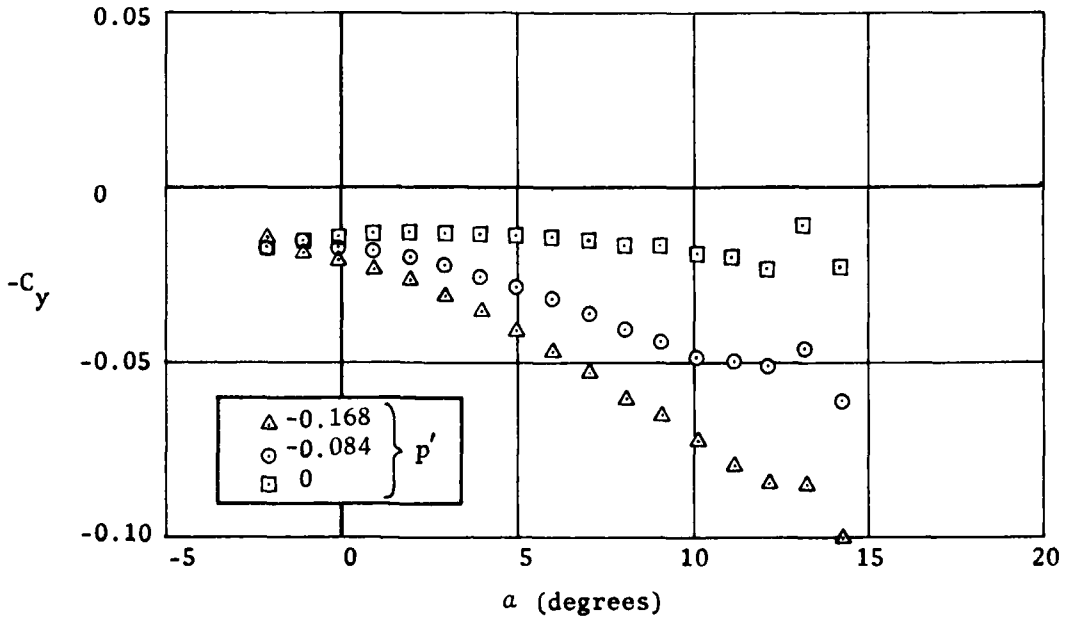

(f) M=0.9, with canards, $\delta_z = \delta_y = 0^o$

Figure 7(Contd.). Variation of side force coefficient with incidence, Mach No. and spin rate

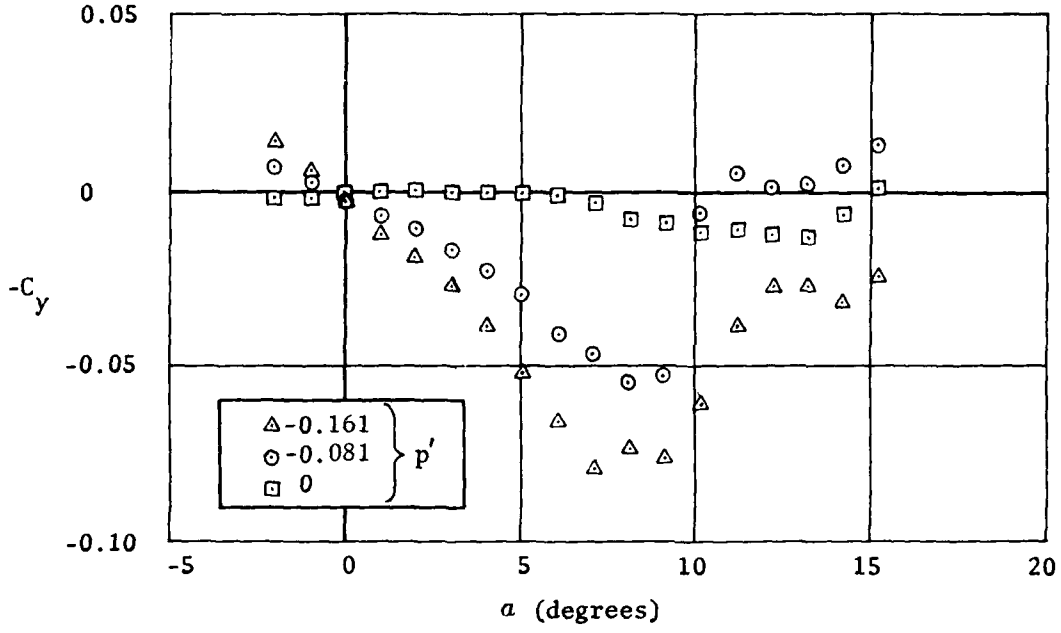

(g) M=0.95, no canards

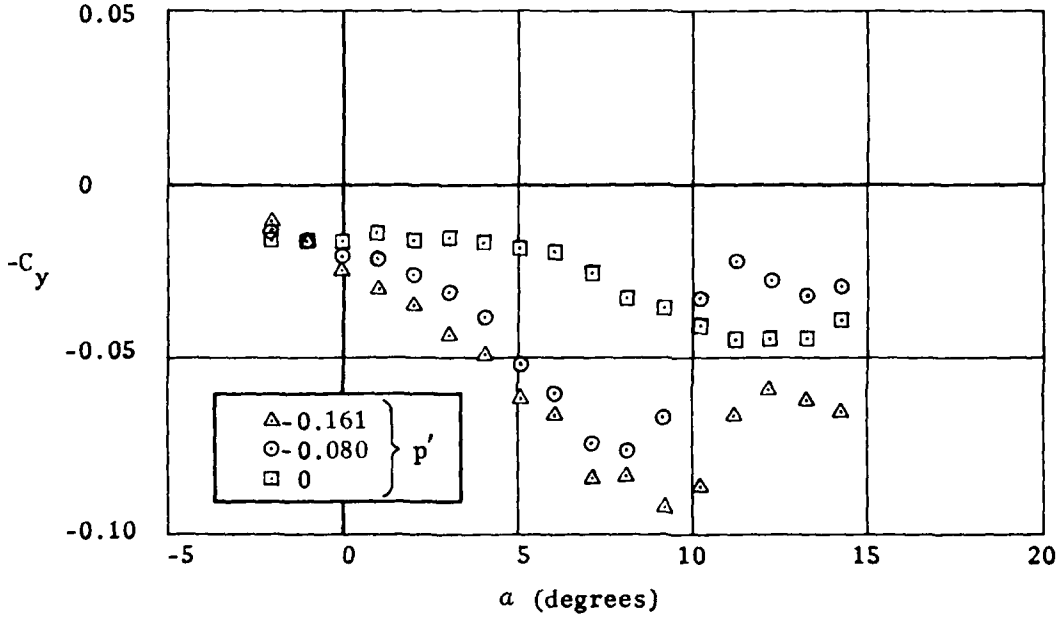

(h) M=0.95, with canards, $\delta_z = \delta_y = 0^o$

Figure 7(Contd.). Variation of side force coefficient with incidence, Mach No. and spin rate

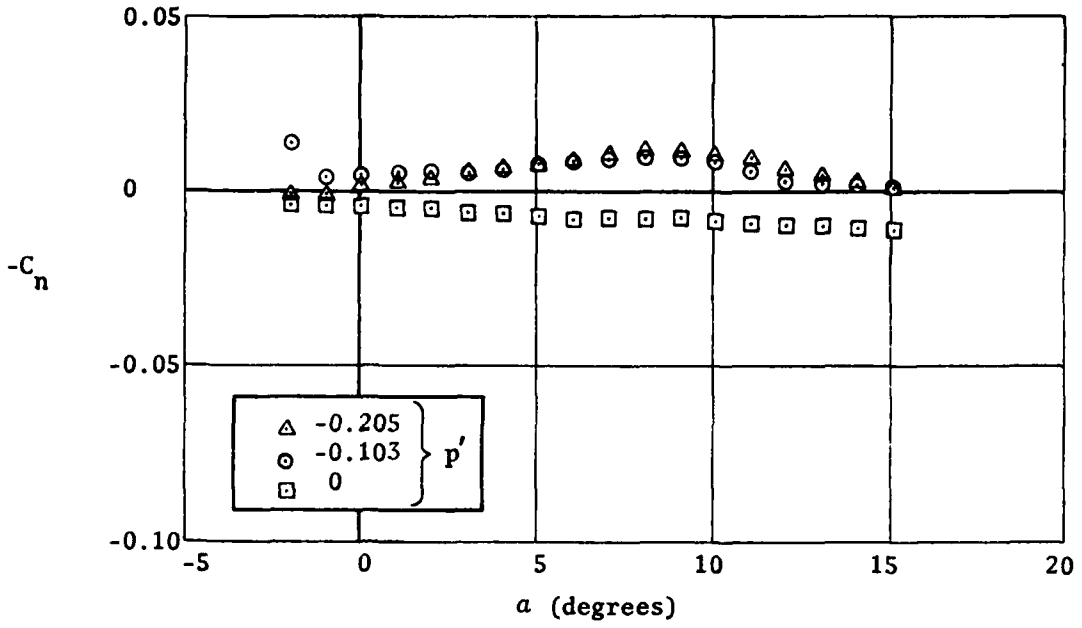

(a) M=0.7, no canards

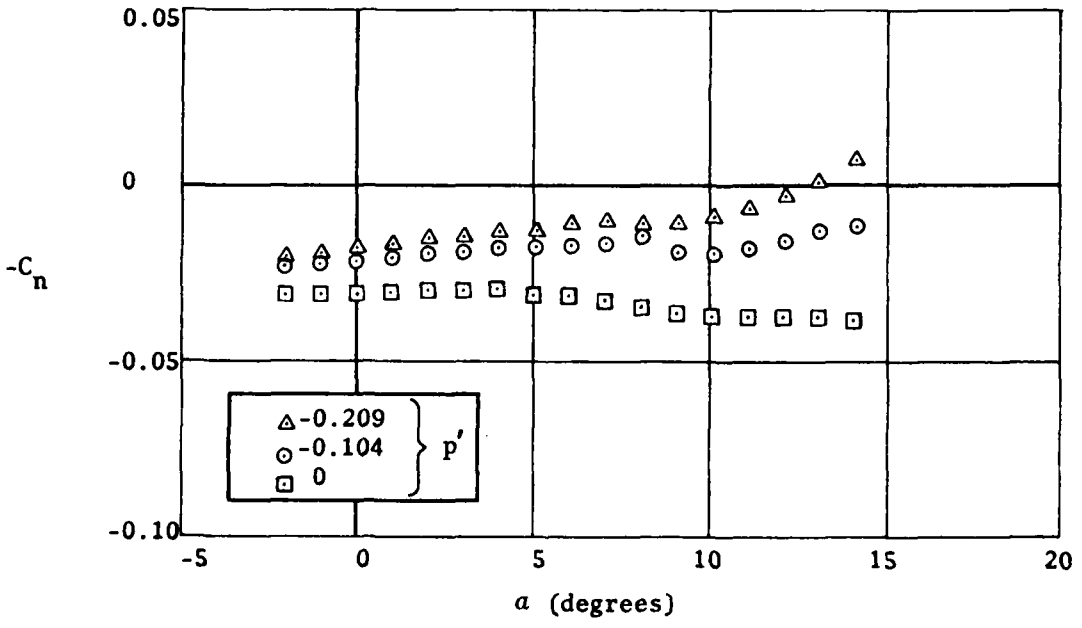

(b) M=0.7, with canards, $\delta_z = \delta_y = 0^o$

Figure 8. Variation of yawing moment coefficient with incidence, Mach No. and spin rate

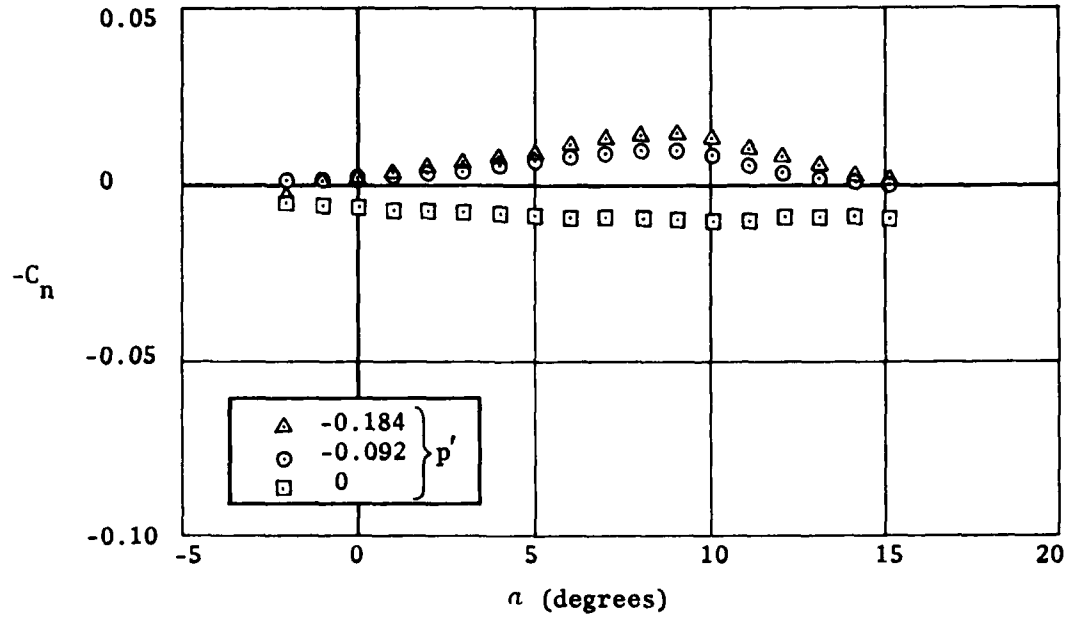

(c) M=0.8, no canards

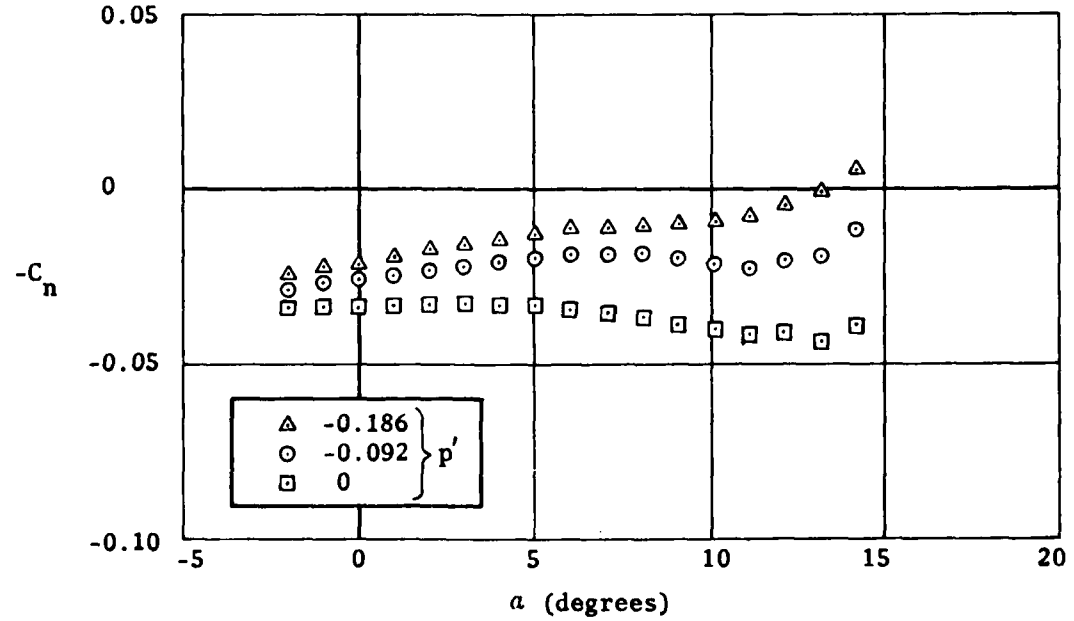

(d) M=0.8, with canards, $\delta_z = \delta_y = 0^o$

Figure 8(Contd.). Variation of yawing moment coefficient with incidence, Mach No. and spin rate

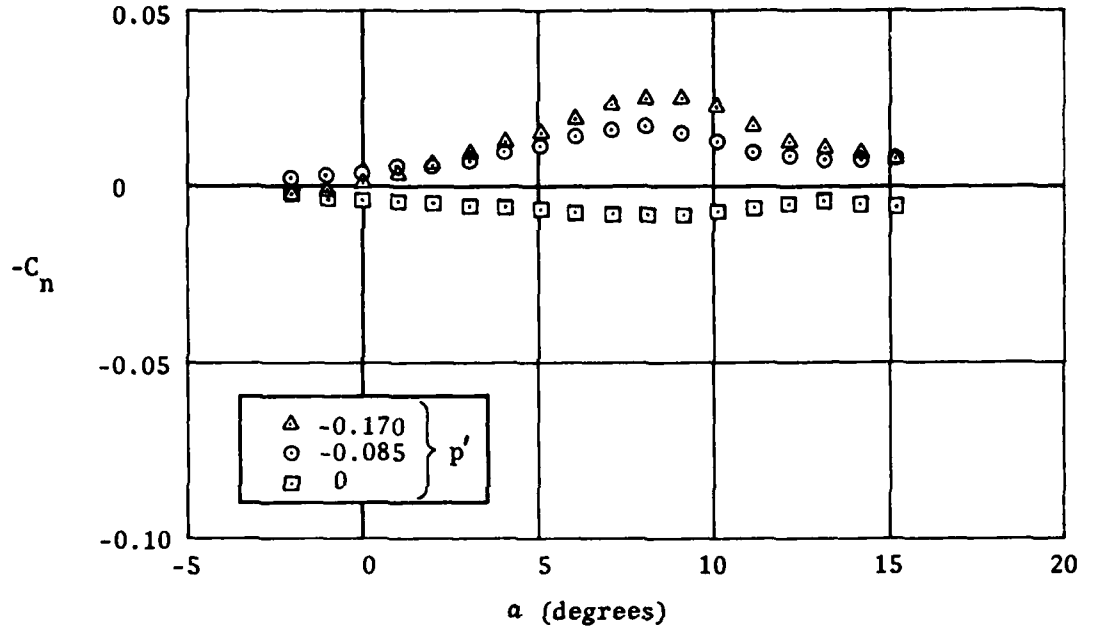

(e) M=0.9, no canards

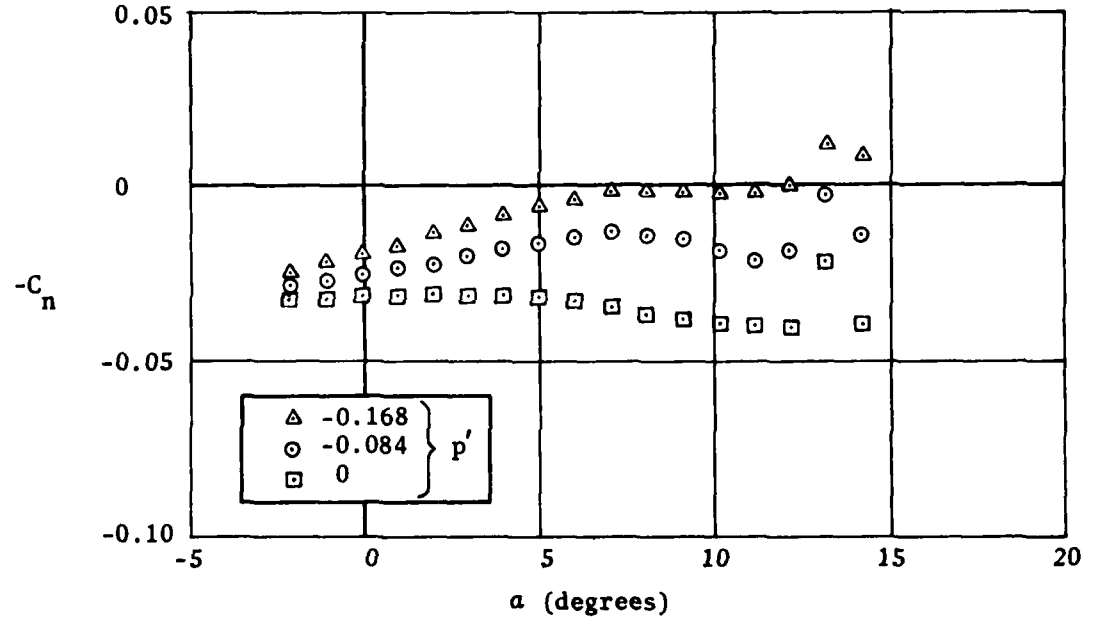

(f) M=0.9, with canards, $\delta_z = \delta_y = 0^o$

Figure 8(Contd.). Variation of yawing moment coefficient with incidence, Mach No. and spin rate

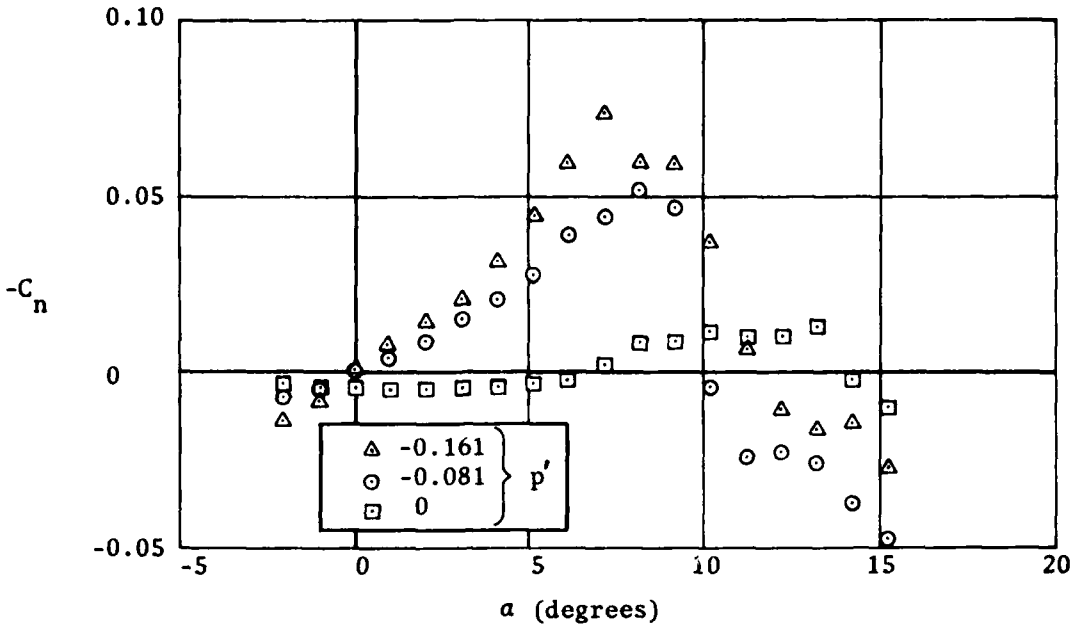

(g) M=0.95, no canards

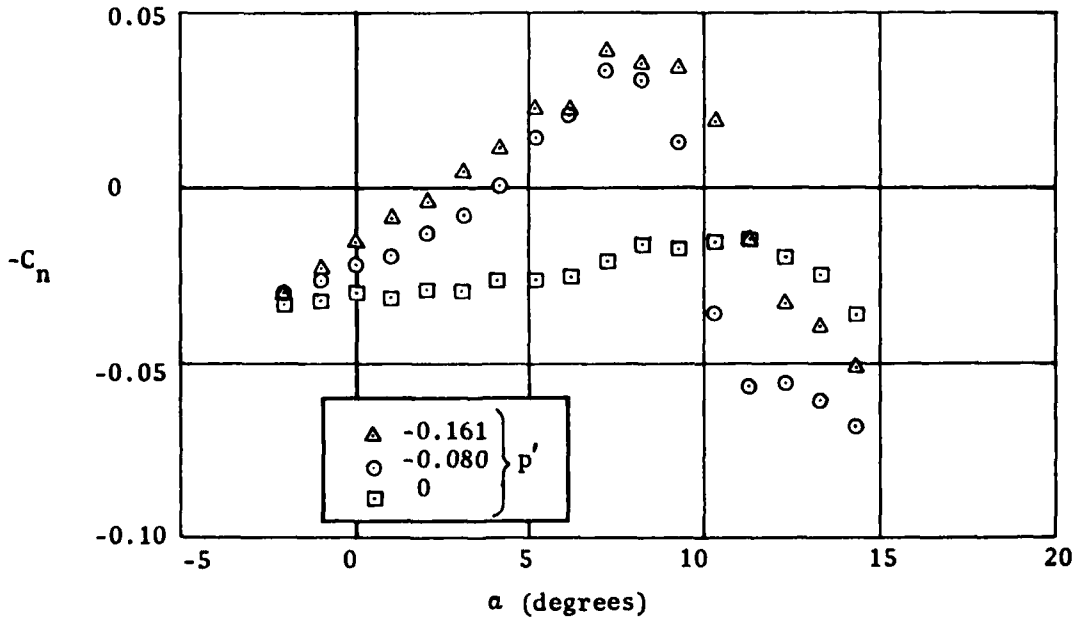

(h) M=0.95, with canards, $\delta_z = \delta_y = 0^o$

Figure 8(Contd.). Variation of yawing moment coefficient with incidence, Mach No. and spin rate

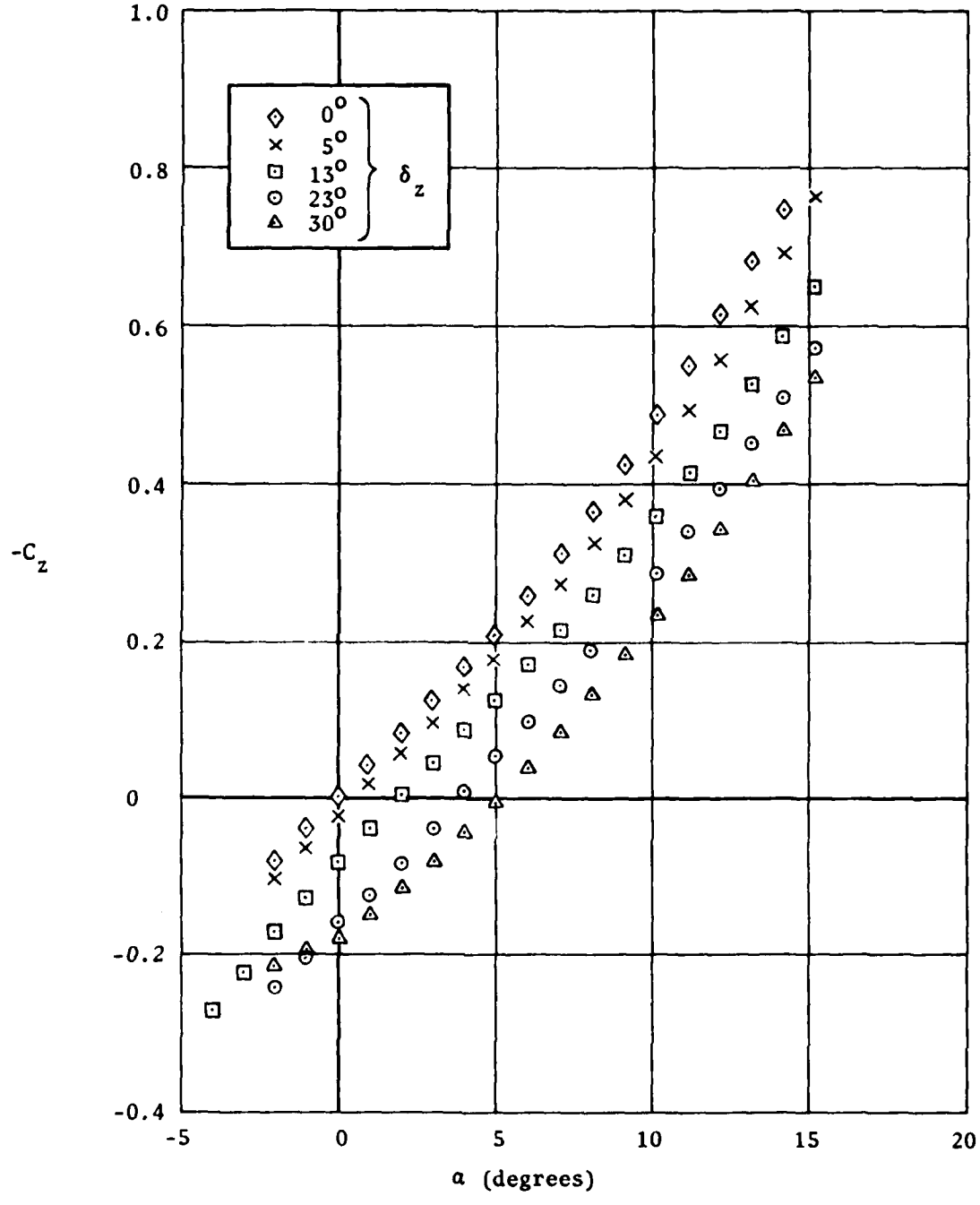

(a) M=0.7

Figure 9. Variation of normal force coefficient with incidence and pitch canard deflection, $p' = 0$, $\delta_y = 0^o$

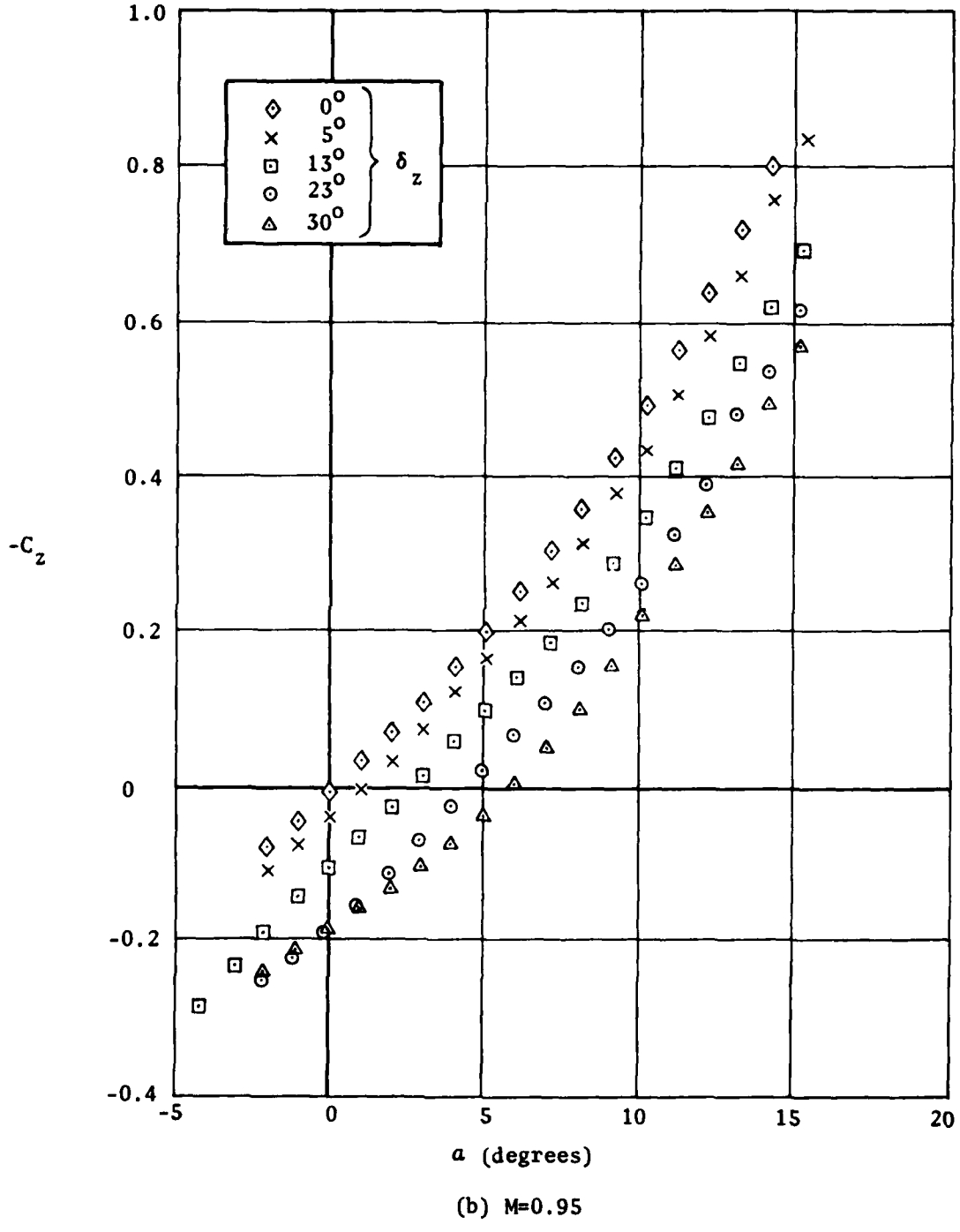

(b) M=0.95

Figure 9(Contd.). Variation of normal force coefficient with incidence and pitch canard deflection, $p' = 0$, $\delta_y = 0^o$

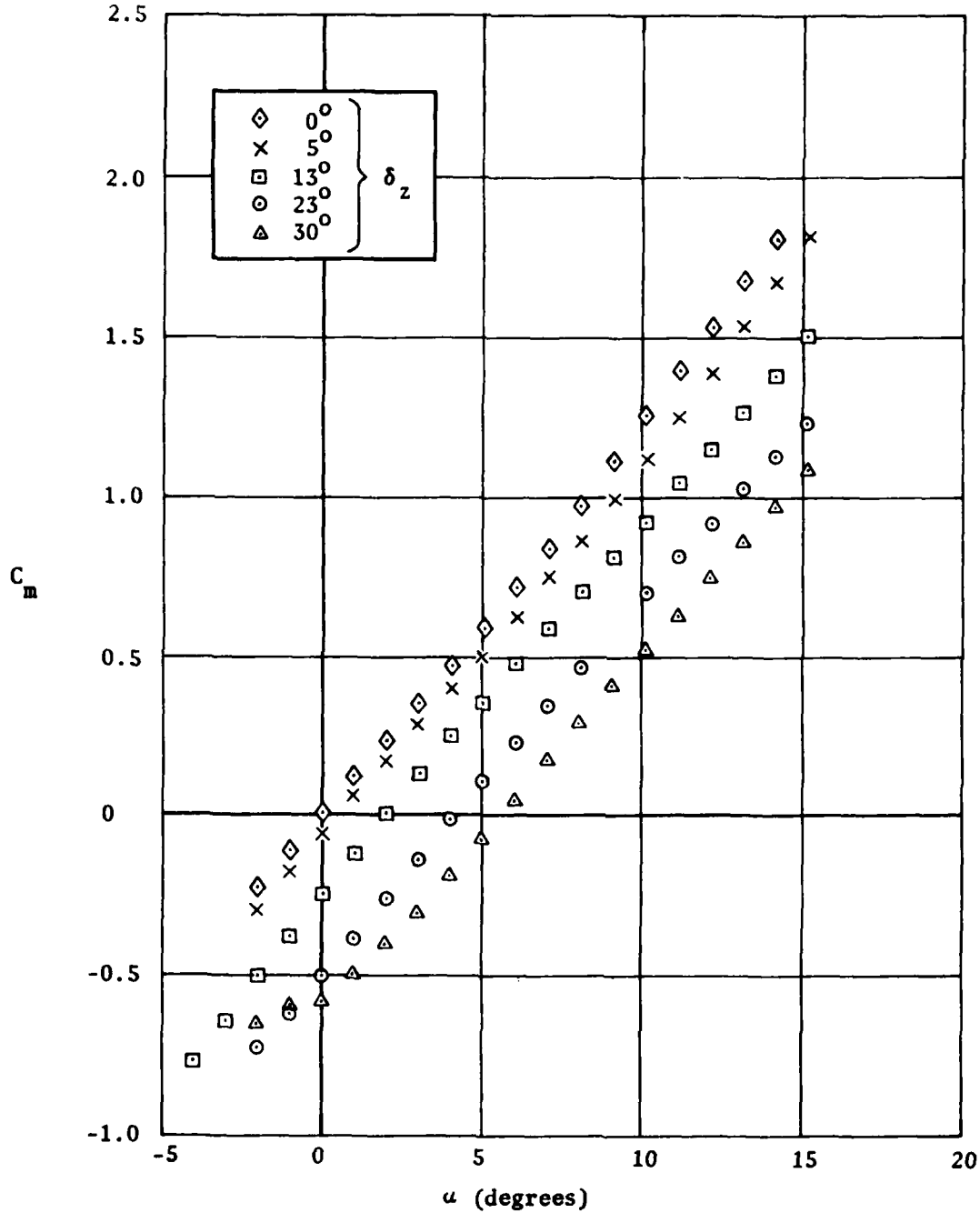

(a) M=0.7

Figure 10. Variation of pitching moment coefficient with incidence and pitch canard deflection, $p' = 0$, $\delta_y = 0^o$

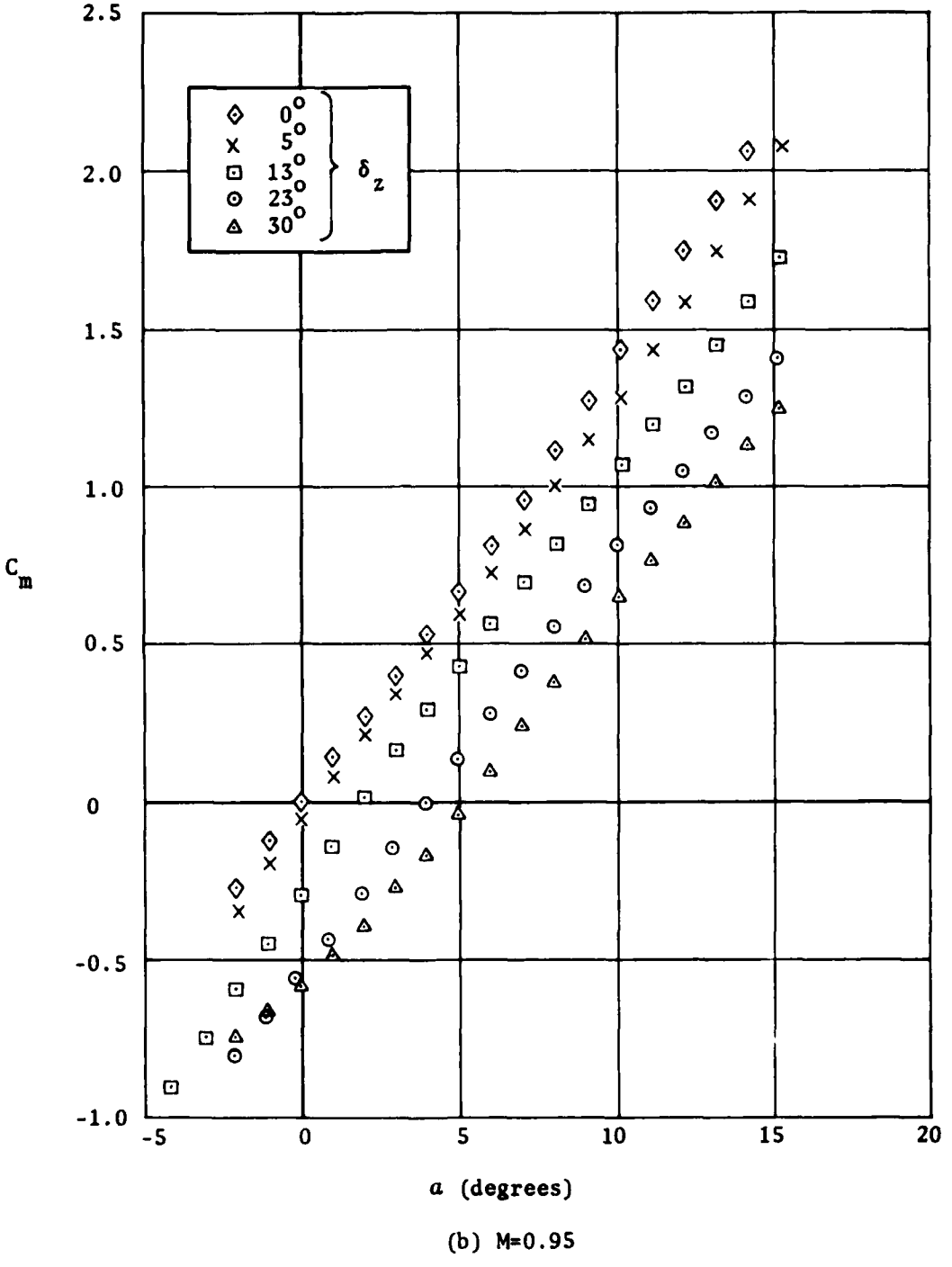

(b) M=0.95

Figure 10(Contd.). Variation of pitching moment coefficient with incidence and pitch canard deflection, $p' = 0$, $\delta_y = 0^o$

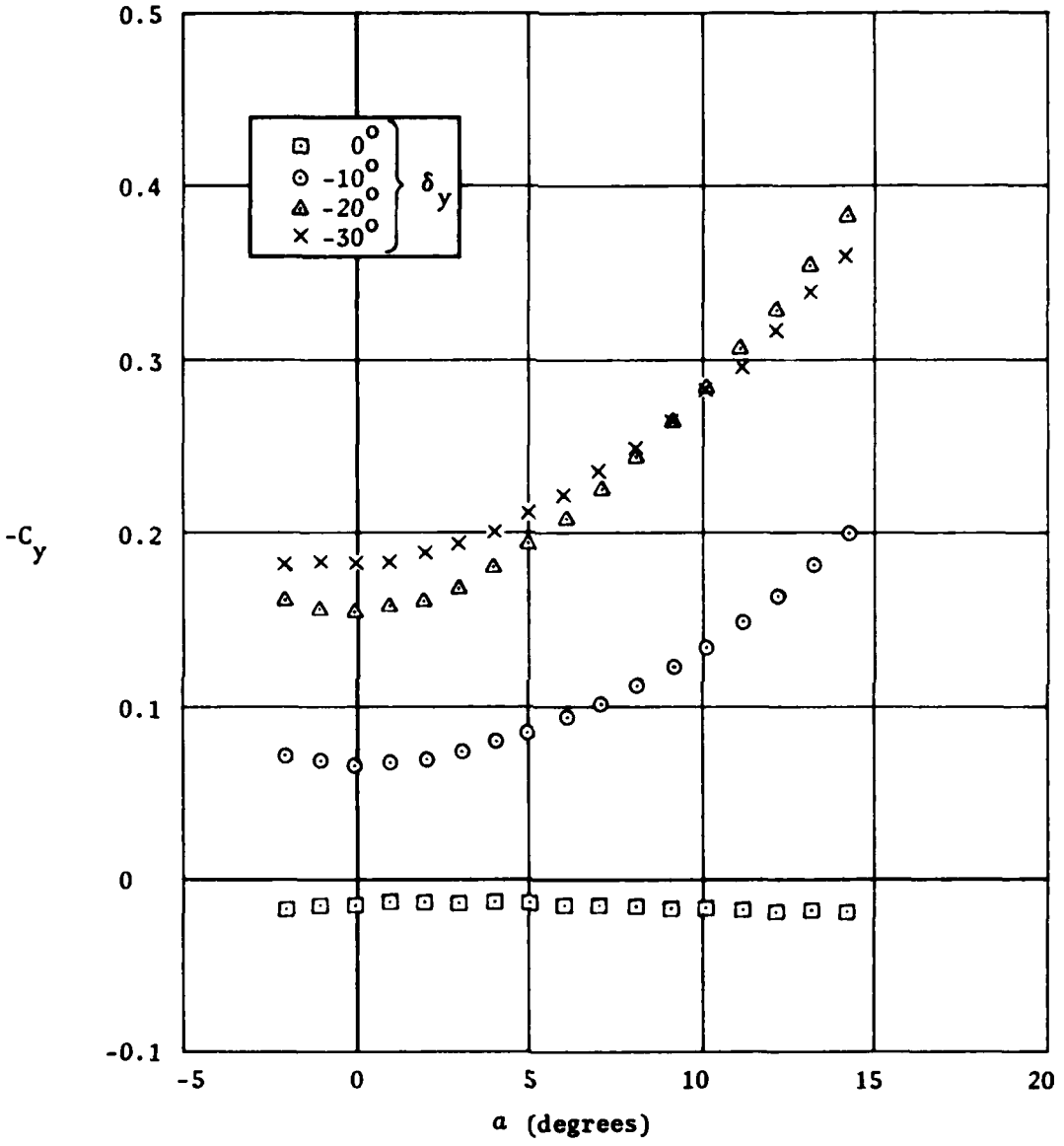

(a) M=0.7

Figure 11. Variation of side force coefficient with incidence and yaw canard deflection, $p' = 0$, $\delta_z = 0^o$

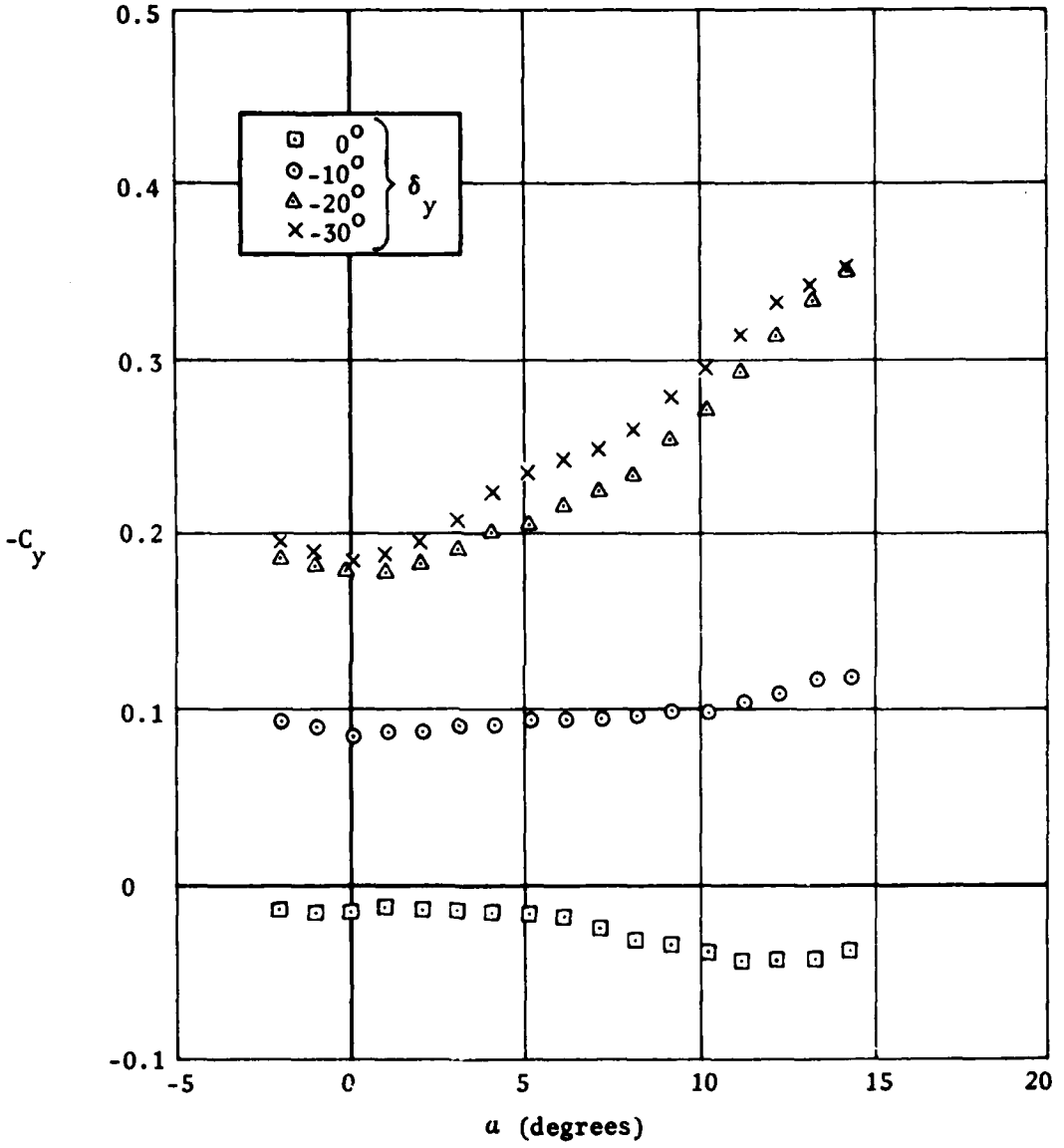

(b) M=0.95

Figure 11(Contd.). Variation of side force coefficient with incidence and yaw canard deflection, $p' = 0^o$, $\delta_z = 0^o$

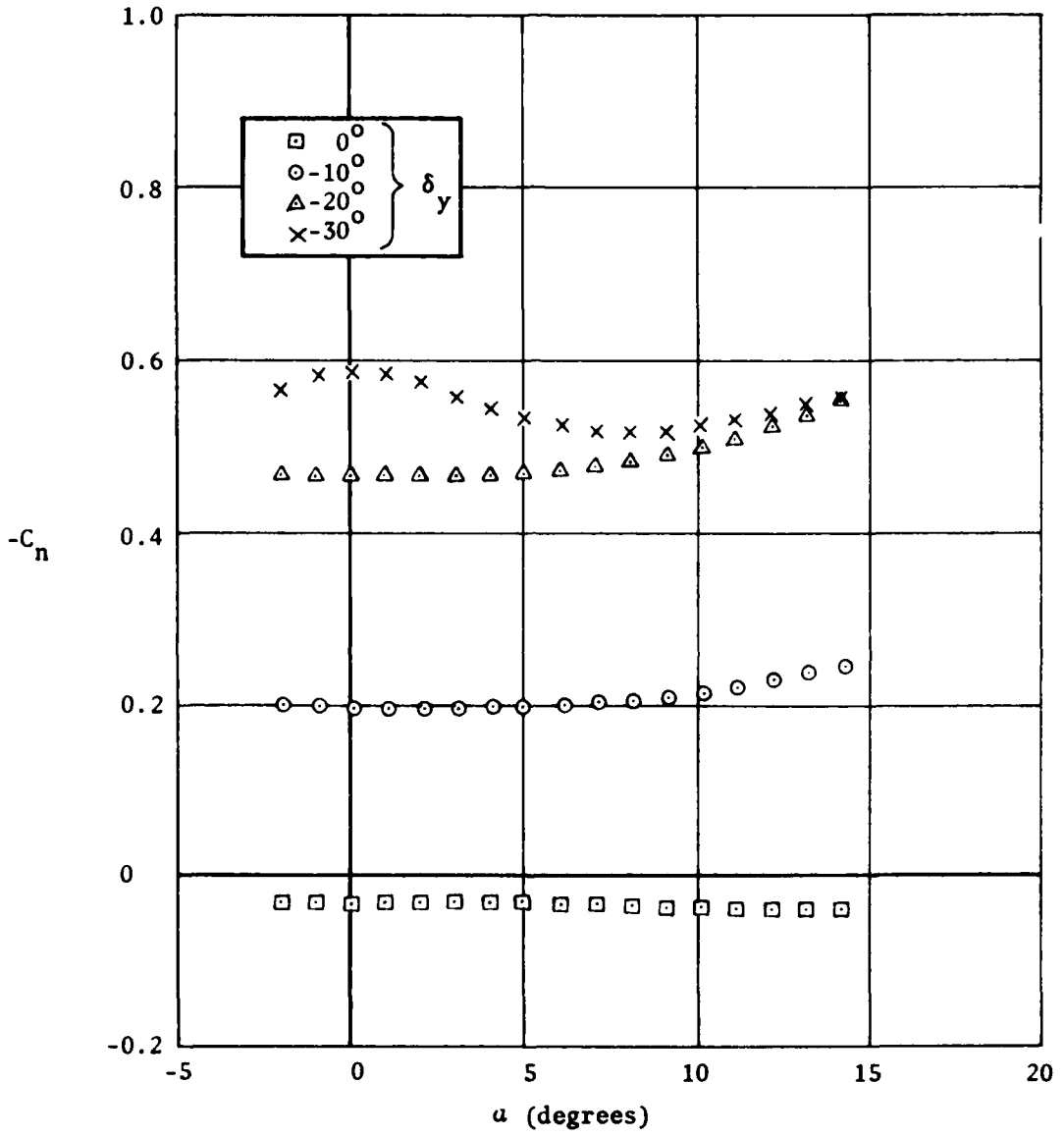

(a) M=0.7

Figure 12. Variation of yawing moment coefficient with incidence and yaw canard deflection, $p' = 0$, $\delta_z = 0^o$

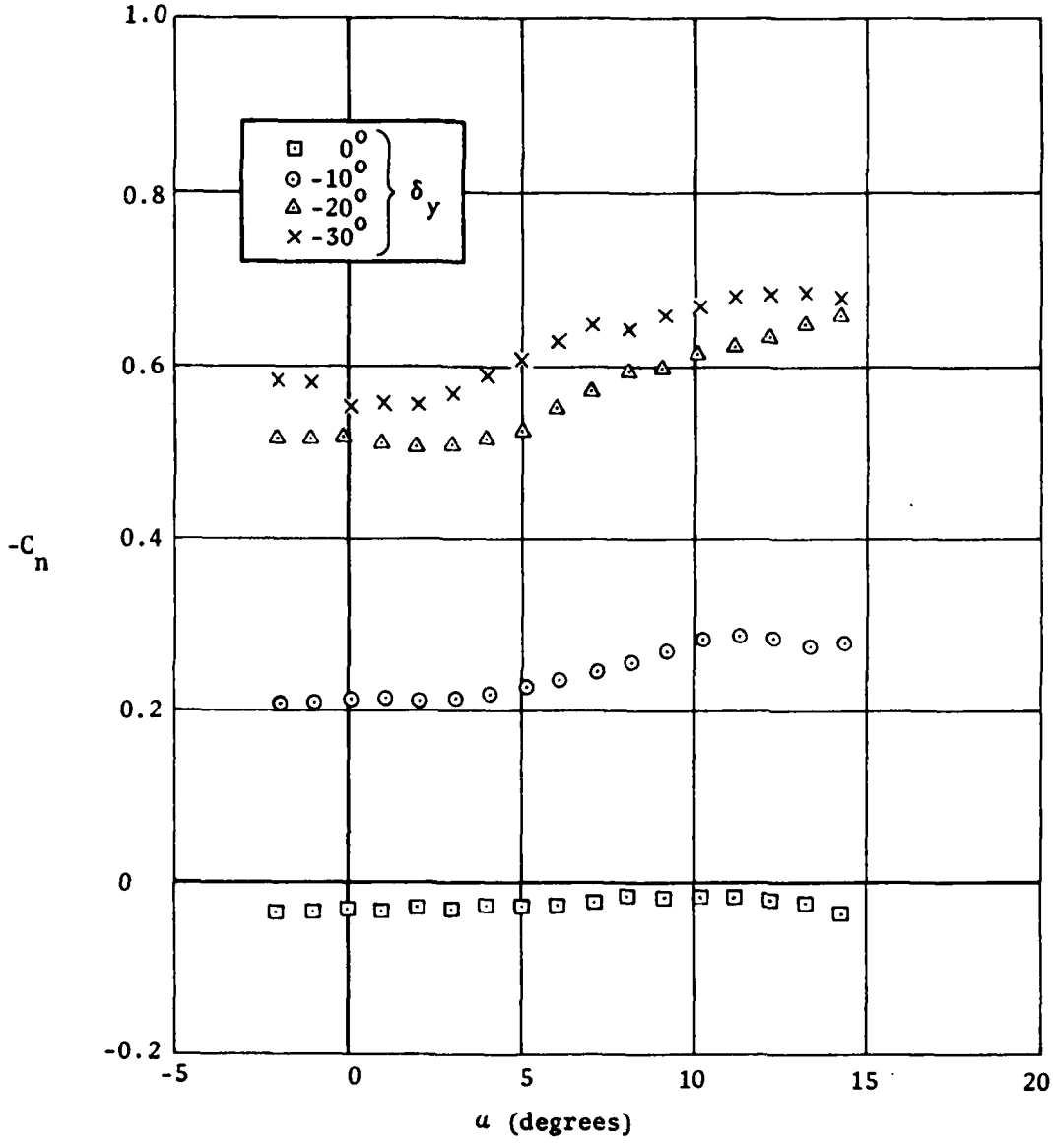

(b) M=0.95

Figure 12(Contd.). Variation of yawing moment coefficient with incidence and yaw canard deflection, $p' = 0$, $\delta_z = 0^o$

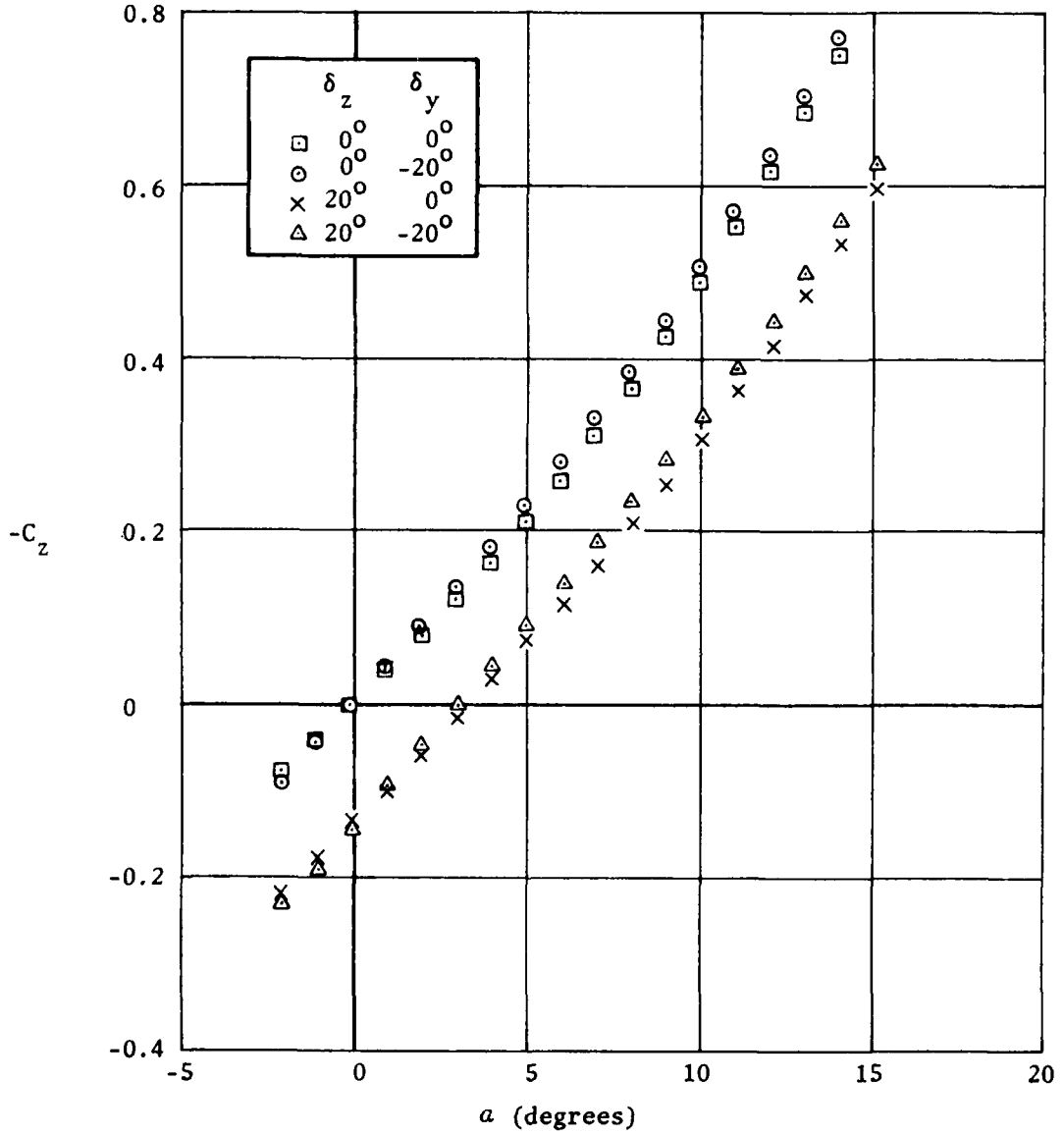

(a) Normal force coefficient

Figure 13. Variation of aerodynamic coefficients with incidence, showing effect of pitch and yaw canard deflections applied separately and in combination, M = 0.7, $p' = 0$

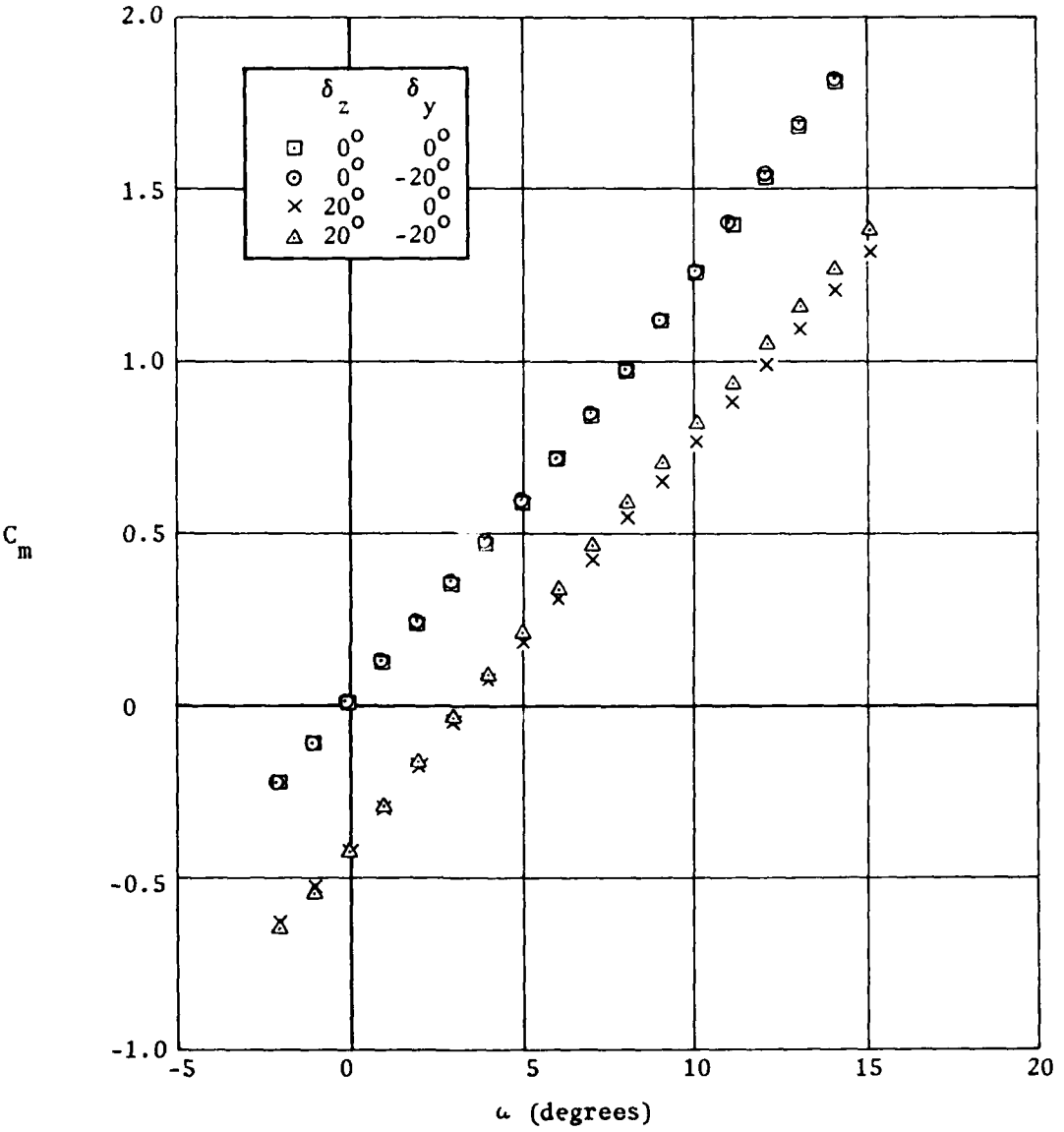

(b) Pitching moment coefficient

Figure 13(Contd.). Variation of aerodynamic coefficients with incidence, showing effect of pitch and yaw canard deflections applied separately and in combination, M = 0.7, $p' = 0$

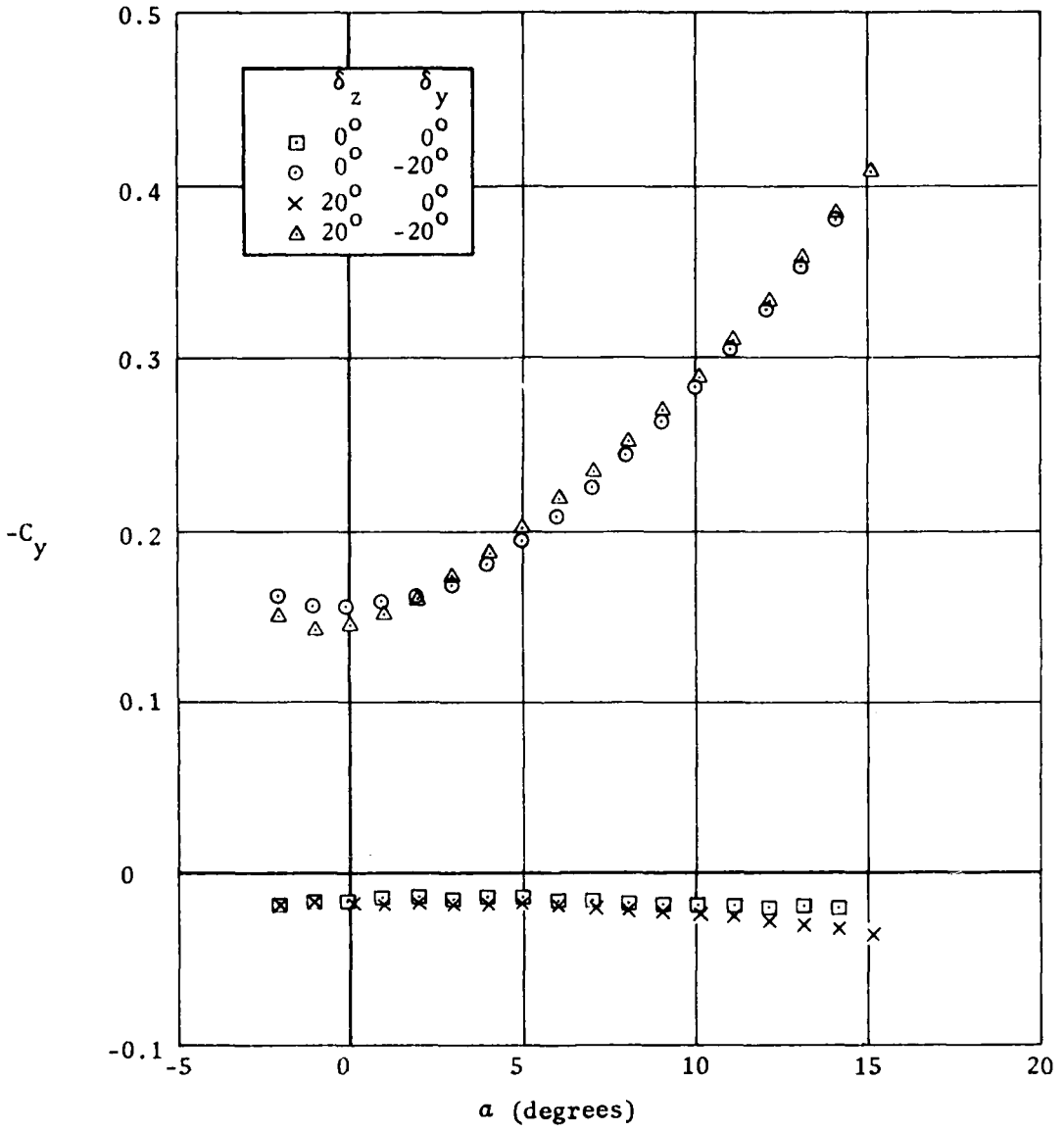

(c) Side force coefficient

Figure 13(Contd.). Variation of aerodynamic coefficients with incidence, showing effect of pitch and yaw canard deflections applied separately and in combination, M = 0.7, $p' = 0$

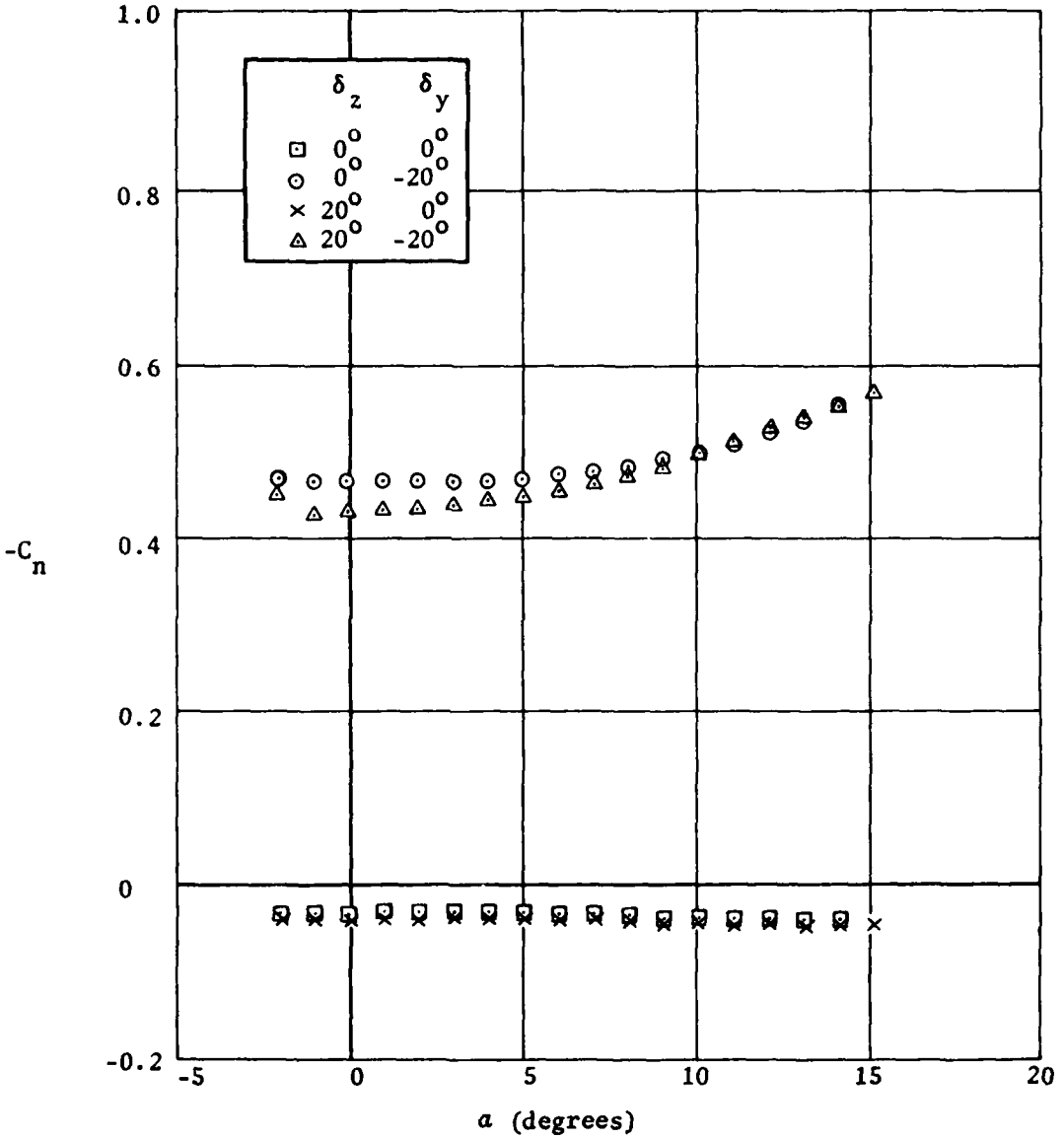

(d) Yawing moment coefficient

Figure 13(Contd.). Variation of aerodynamic coefficients with incidence, showing effect of pitch and yaw canard deflections applied separately and in combination, M = 0.7, $p' = 0$

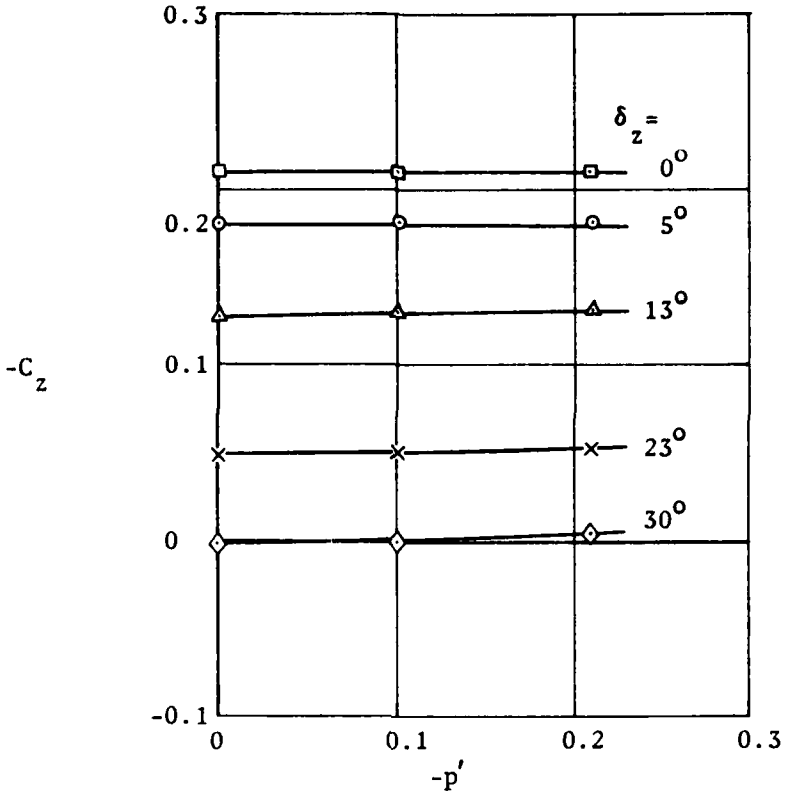

(a) Normal force coefficient, $\delta_y = 0^\circ$

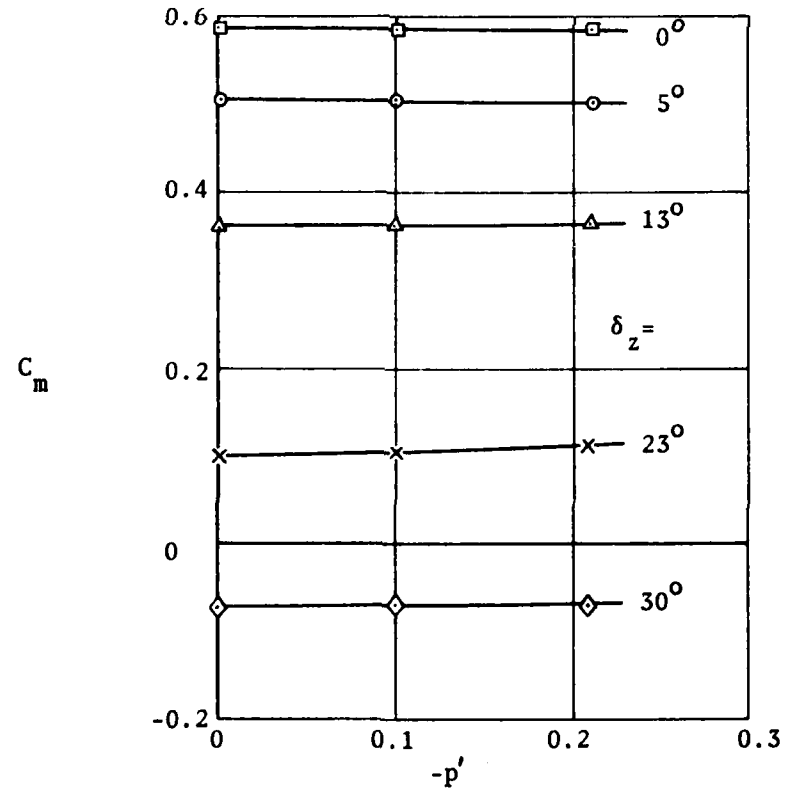

(b) Pitching moment coefficient, $\delta_y = 0^\circ$

Figure 14. Variation of aerodynamic coefficients with spin rate, showing effect of pitch and yaw canard deflections, M = 0.7, $\alpha = 5^\circ$

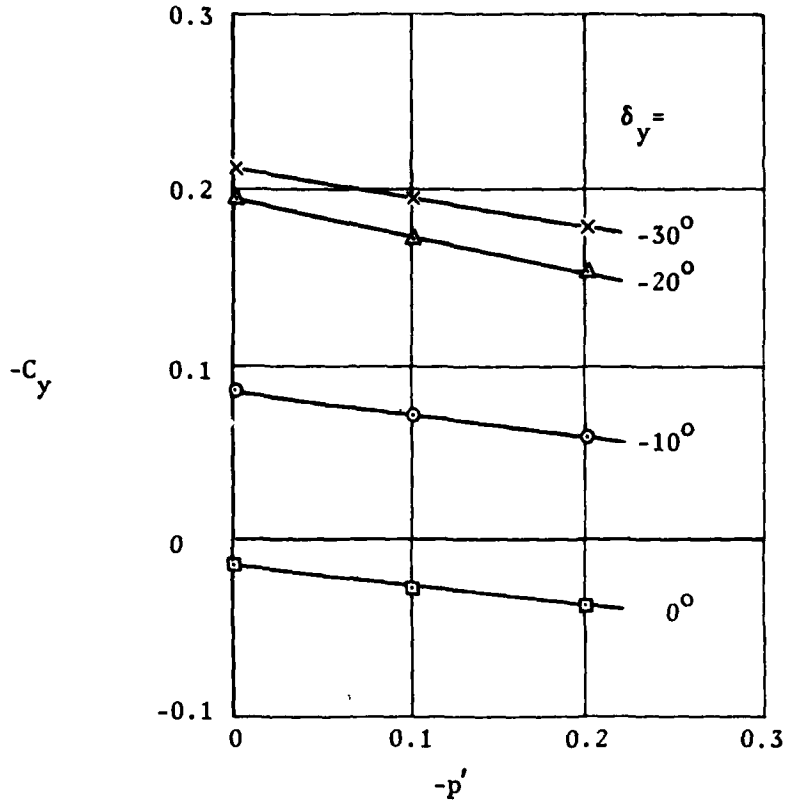

(c) Side force coefficient, $\delta_z = 0^\circ$

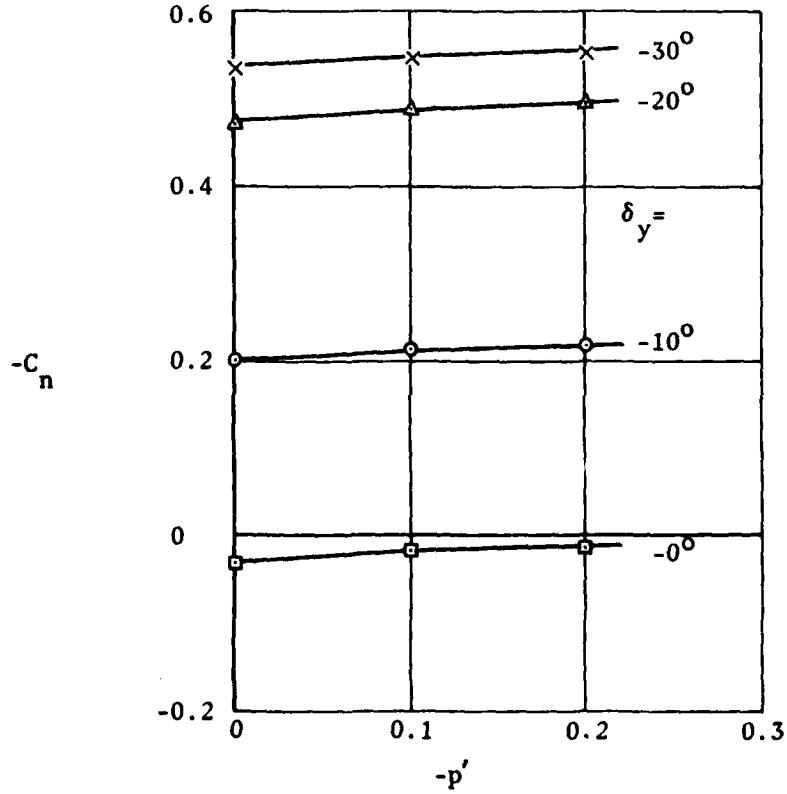

(d) Yawing moment coefficient, $\delta_z = 0^\circ$

Figure 14(Contd.). Variation of aerodynamic coefficients with spin rate, showing effect of pitch and yaw canard deflections, M = 0.7, $\alpha = 5^\circ$

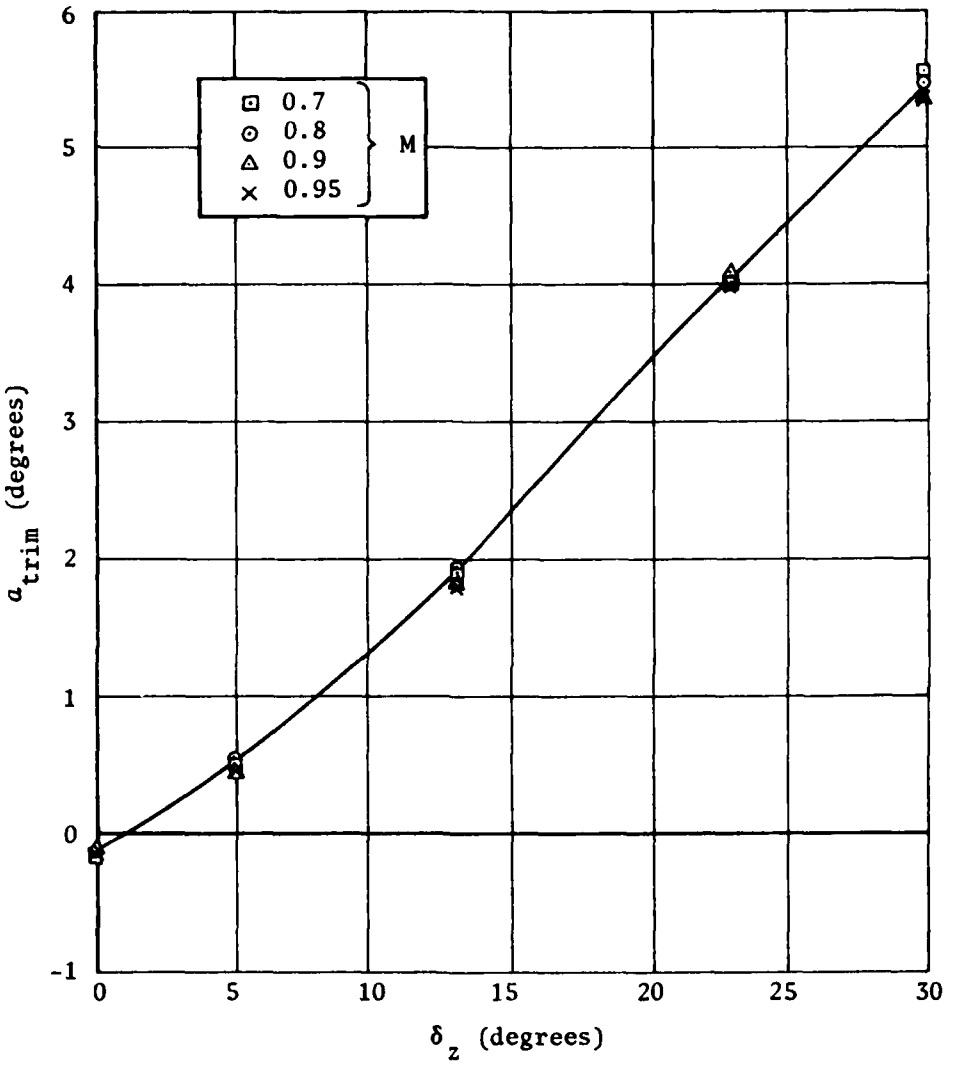

Figure 15. Variation of trim incidence with pitch canard deflection and Mach No., $p' = 0$, $\delta_y = 0^0$

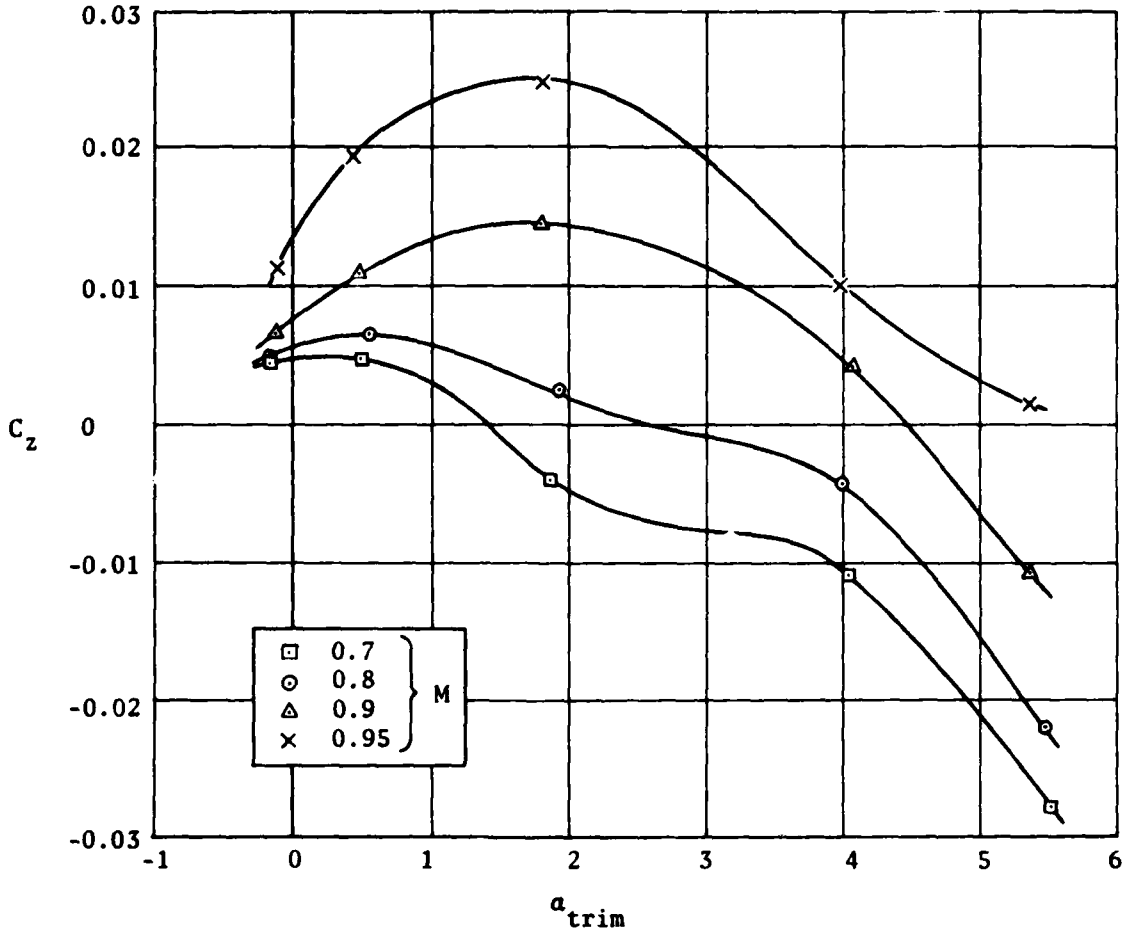

(a) Normal force coefficient, $p' \approx 0$

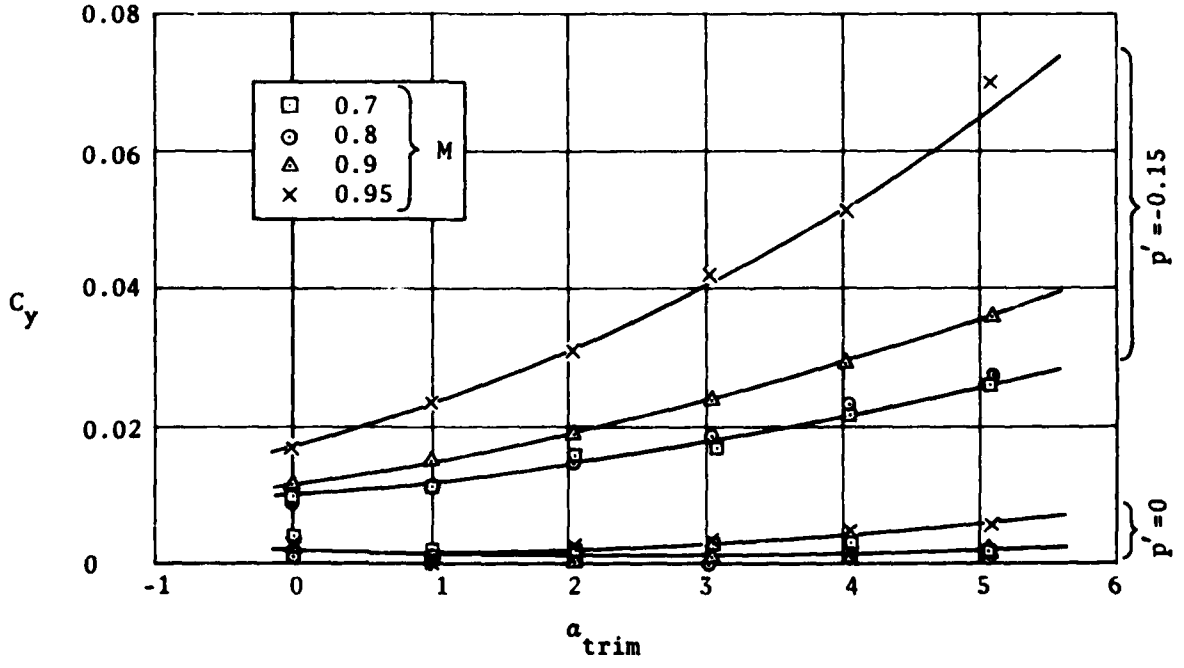

(b) Side force coefficient

Figure 16. Variation of normal force and side force coefficients with trim incidence and Mach No.

DISTRIBUTION

	Copy No.
EXTERNAL	
In United Kingdom	
Defence Scientific and Technical Representative, London	1
TTCP UK National Leader, Technical Panel W-2	2 - 5
British Library Lending Division Boston Spa Yorks, U.K.	6
In United States of America	
TTCP US National Leader, Technical Panel W-2	7 - 10
Counsellor, Defence Science, Washington	11
NASA Scientific and Technical Information Office, Washington	12
National Technical Information Services, Springfield Va 22151, U.S.A.	13
Engineering Societies Library New York NY 10017, U.S.A.	14
In Canada	
TTCP Canadian National Leader, Technical Panel W-2	15 - 18
In Australia	
Chief Defence Scientist	19
Deputy Chief Defence Scientist	20
Director, Joint Intelligence Organisation (DDSTI)	21
Controller, Programmes and Analytical Studies	22
Navy Scientific Adviser	23 - 24
Army Scientific Adviser	25 - 26
Air Force Scientific Adviser	27 - 28
Superintendent, Major Projects	29
Superintendent, Science and Technology Programmes	30
Controller, Service Laboratories and Trials Division	31
Superintendent, RAN Research Laboratory	32
Head, Engineering Development Establishment	33
Defence Information Services Branch (for microfilming)	34
Defence Information Services Branch for:	
United Kingdom, Ministry of Defence, Defence Research Information Centre (DRIC)	35
United States, Department of Defense, Defense Documentation Center	36 - 47
Canada, Department of National Defence, Defence Science Information Service	48
New Zealand, Ministry of Defence	49
Australian National Library	50

	Copy No.
Defence Library, Campbell Park	51
Library, Aeronautical Research Laboratories	52
Library, Materials Research Laboratories	53
WITHIN DRCS	
Chief Superintendent, Weapons Systems Research Laboratory	54
Chief Superintendent, Advanced Engineering Laboratory	55
Chief Superintendent, Electronics Research Laboratory	56
Superintendent, Aeroballistics Division	57
Superintendent, Weapon Systems Division	58
Superintendent, Communications and Electronic Engineering Division	59
Superintendent, Workshops and Mechanical Design Division	60
Superintendent, Electronic Warfare Division	61
Principal Engineer, Air Weapons Engineering	62
Senior Principal Research Scientist, Ballistics	63
Principal Officer, Aerodynamics Research Group	64
Mr M.L. Robinson, Aerodynamics Research Group	65
Mr C.E. Fenton, Aerodynamics Research Group	66
Principal Officer, Dynamics Group	67
Principal Officer, Flight Research Group	68
Mr K.H. Lloyd, Flight Research Group	69
Dr D.P. Brown, Flight Research Group	70
Principal Officer, Ballistic Studies Group	71
Mr A.M. Sayer, Ballistics Studies Group	72
Principal Officer, Field Experiments Group	73
Principal Officer, Terminal Guidance Group	74
Author	75 - 76
DRCS Library	77 - 78
AD Library	79 - 80
Spares	81 - 84


DATE
ILMED
8